

Original Article

WHO DRIVES THE PROGRESS OF OSTEOARTHRITIS? - A DESCRIPTIVE STUDY OF SYNOVIUM-MENISCUS CROSSTALK

F. Yu^{1,2,3,§}, T.T. Qi^{1,2,3,§}, J. Weng^{1,2,3}, T.B. Wang⁴, P. Liu^{1,2,3}, Y.Q. Chen^{1,2,3}, A. Xiong^{1,2,3},
D.L. Wang^{1,2,3,*} and H. Zeng^{1,2,3,5,*}

¹Department of Bone & Joint Surgery, Peking University Shenzhen Hospital, Shenzhen Peking University-The Hong Kong University of Science and Technology Medical Center, 518036 Shenzhen, Guangdong, China

²National & Local Joint Engineering Research Center of Orthopaedic Biomaterials, 518036 Shenzhen, Guangdong, China

³Shenzhen Key Laboratory of Orthopaedic Diseases and Biomaterials Research, 518036 Shenzhen, Guangdong, China

⁴Department of Orthopedics and Trauma, Peking University People's Hospital, 100044 Beijing, China

⁵Department of Orthopedics, Shenzhen Second People's Hospital, 518000 Shenzhen, Guangdong, China

[§]These authors contributed equally.

Abstract

Objective: The incidence of osteoarthritis (OA) increases with each passing year. The degeneration of the meniscus and synovium is considered the initial factor of knee osteoarthritis (KOA), but their synergistic mechanism has not been clarified. **Methods:** In this study, single-cell RNA sequencing (scRNA-seq) was employed to establish 16 normal or degenerated meniscus samples and 6 synovium samples based on the meniscus and synovium tissues of 16 patients. A cell atlas comprising 124,026 single cells in total was established (including 8 patients from the public database The Genome Sequence Archive for Human (GSA-Human) PRJCA008120). **Results:** Based on the exploration of the meniscus/synovium microenvironment homeostasis and the crosstalk between them during their degeneration, this study provided a comprehensive description of the involved cellular interactions. The cell types present in the meniscus and synovium were analyzed, and new fibroblast subtypes related to their degeneration were identified. Additionally, the interactions within pathways such as vascular endothelial growth factor (VEGF) and VISFATIN between the meniscus and synovium were studied, with a focus on various cell subtypes. The mechanisms involving vascular growth, immune cell infiltration, and common or distinct genes during the degeneration of synovium and meniscus tissues were also investigated. **Conclusion:** This study presented the largest cellular atlas of the synovium and meniscus in osteoarthritis (OA) to date, reflecting a detailed description of the cellular crosstalk during degeneration. The findings suggested that the synovium played a significant role in the intra-articular tissue crosstalk (synovium/meniscus), thereby contributing to the degeneration observed in OA.

Keywords: Osteoarthritis, crosstalk, synovium, meniscus, single-cell RNA sequencing.

***Address for correspondence:** D.L. Wang, Department of Bone & Joint Surgery, Peking University Shenzhen Hospital, Shenzhen Peking University-The Hong Kong University of Science and Technology Medical Center, 518036 Shenzhen, Guangdong, China. Email: wangdelinavy@163.com; H. Zeng, Department of Bone & Joint Surgery, Peking University Shenzhen Hospital, Shenzhen Peking University-The Hong Kong University of Science and Technology Medical Center, 518036 Shenzhen, Guangdong, China. Email: zenghui@pkusz.com.

Copyright policy: © 2024 The Author(s). Published by Forum Multimedia Publishing, LLC. This article is distributed in accordance with Creative Commons Attribution Licence (<http://creativecommons.org/licenses/by/4.0/>).

Introduction

Osteoarthritis (OA) is a chronic disease related to the degeneration of articular cartilage tissues, involving the total joint that may affect the synovium, meniscus, cartilage, subchondral bone, ligament, and muscle of patients. Synovial fibroblasts and meniscus chondrocytes are considered the most abundant and widely distributed cells with the most significant direct correlation with the degenerative process (Chou *et al.*, 2020; Fu *et al.*, 2022; Sun *et al.*,

2020). Synovium and meniscus/cartilage samples from OA patients have been analyzed separately in many previous studies (Fu *et al.*, 2022; Zhang *et al.*, 2019), and fibroblasts have been divided into different subtypes. Based on previous studies on the single cell in the cartilage, Fu *et al.* (2022) divided meniscus cells in OA into five subtypes, comprising Ch.1 (*CHAD*), Ch.2 (*FNDC1*), Ch.3 (*PRG4*), Ch.4 (*CFD*), and Ch.5 (cycling). Zhang *et al.* (2019) defined synovial lining fibroblasts (*PDPN* and *PRG4*) and synovial sublining fibroblasts (*PDPN* and *THY1*), which

was different from Wei's definition of synovial lining fibroblasts (*PRG4*, *PDGFRA*, and *PDPN*) and synovial sublining fibroblasts (*THY1*, *PDGFRA*, and *PDPN*) (Wei *et al.*, 2020). On this basis, Micheroli *et al.* (2022) further explored a new subtype of *CXCL14*⁺ synovial fibroblasts (*CXCL14*, *C3*, *CD34*, *ASPN*, and *THY1*) with high expression of *CXCL14*.

Through single-cell studies of the synovium and cartilage, it can be found that synovial fibroblasts and meniscus chondrocytes have similar characteristics, functions, and marker genes, such as *PRG4*, *HTRAI*, *CD55*, *COL3A1*, *STMN1*, and *MMP2* (Chou *et al.*, 2020; Fu *et al.*, 2022; Ji *et al.*, 2019; Sun *et al.*, 2020). Moreover, fibrochondrocytes (FCs) (Ji *et al.*, 2019; Sun *et al.*, 2020) and *PRG4*⁺ chondrocytes (Ch.3) (Fu *et al.*, 2022) with the characteristics of fibroblasts have also been identified in single-cell studies based on the cartilage samples from OA patients. The close relationship between these two kinds of cells has also been verified in previous studies (Song *et al.*, 2015; Sakaguchi *et al.*, 2005). The co-culture of fibroblasts and chondrocytes can promote cell proliferation and collagen synthesis (Song *et al.*, 2015). Besides, synovial mesenchymal stem cells (SSCs) are superior to mesenchymal stem cells derived from other tissues in forming cartilage tissues (Sakaguchi *et al.*, 2005). SSCs also play a therapeutic role in meniscus defect models of large animals such as pigs (Hatsushika *et al.*, 2014). In addition, some experiments focus on the characteristics of synovial fibroblasts of chondrocytes. It has been demonstrated that the phenotype of chondrogenic progenitor cells (CPCs) is closer to synoviocytes than chondrocytes (Zhou *et al.*, 2014). Compared with relatively static chondrocytes, CPCs may be more similar in phenotype and function to synoviocytes that migrate and proliferate during joint injury (García-Arnandis *et al.*, 2010). Of note, the synovial environment may induce synovial differentiation of chondrocytes. When rat chondrocyte pellets were cultured with synovium-conditioned media, the expression of articular surface marker lubricin proteoglycan 4 (*PRG4*) was significantly induced (Chau *et al.*, 2022). It can be speculated that synovial fibroblasts and meniscus chondrocytes may be cells with similar tissue homology and thus play a synergistic role.

In this study, the cellular association between synovium and meniscus samples was systematically revealed. A transcriptomic atlas of 124,026 cells was generated from 22 normal/degenerative meniscus samples from 16 donors. To the best of our knowledge, this may be a single-cell RNA sequencing (scRNA-seq)-based study with the largest sample size and cell size based on synovium and meniscus samples from OA patients. Besides, the first dataset based on the integrative analysis of meniscus and synovium samples was constructed. In addition, the crosstalk, differentially expressed genes (DEGs), and pseudotime between normal and degenerated synovium and meniscus samples were also analyzed. Based on that, three new fibroblast subtypes were

identified, including fibrochondrocytes (FCs), Fibroblast_1 (Fib_1), and Fibroblast_2 (Fib_2), respectively. In this study, it was demonstrated that the crosstalk of synovium and meniscus may be closely related to the degeneration in OA. Many subtypes of synoviocytes were involved in this process, which provided a basis for the intervention of early synovial lesions and synovitis in OA.

Methods

Human Sample Preparation

In this study, these 16 patients were composed of 8 patients from Genome Sequence Archive for Human (GSA-Human) (<https://ngdc.cnbc.ac.cn/gsa-human/>) with the accession number PRJCA008120 and 8 inpatients from the Department of Osteoarthritis, Peking University Shenzhen Hospital (**Supplementary Table 1**). Among the 8 patient samples provided by GSA-Human, there were 6 degenerated meniscus samples and 6 normal meniscus samples. Among the 8 patient samples provided by the Department of Osteoarthritis, Peking University Shenzhen Hospital, there were 4 degenerated meniscus samples, 3 degenerated synovium samples, and 3 normal synovium samples. The normal synovium group was composed of the synovial tissues of the knee joint from patients with acute injury-related diseases. The degenerated synovium group and degenerated meniscus group were composed of knee synovium and medial meniscus posterior horn outer (red-red zone) areas from patients with severe osteoarthritis undergoing total knee arthroplasty. 2 patients provided paired synovium and meniscus samples (Donor K provided lateral meniscus samples (K outer) and synovium samples (K Syn); Donor L provided lateral meniscus samples (L outer) and synovium samples (L Syn)). In this study, there were 10 degenerated meniscus samples, 3 degenerated synovium samples, 6 normal meniscus samples, and 3 normal synovium samples. Of note, 6 inner samples from the public database PRJCA008120 were mainly used for early data integration to verify the batch effect of data integration samples. These 6 inner samples (A2inner, B1inner, C1inner, E1inner, F9inner, and H12inner) were not included in the differentially expressed gene (DEG) and scMetabolism analysis system. The 22 samples, consisting of 124,026 cells in total, were included in other analyses. **Supplementary Fig. 2a** presents the details of these samples. In addition, a normal meniscus specimen was taken from a patient with severe trauma and underwent amputation surgery for immunofluorescence (IF) staining.

During sample preparation, the meniscus and synovium were cut into small pieces. Then, digestion and dissociation were performed using 150 U/mL collagenase II (Cat # LS004176, Worthington Biochemical Corporation, Lakewood, NJ, USA), 2 mg/mL collagenase IV (Cat # LS004188, Worthington Biochemical Corporation, Lakewood, NJ, USA), 1.2 U/mL Dispase II (Cat # LS02104, Worthington Biochemical Corporation, Lakewood, NJ,

USA), and 50 U/mL DNase I (Cat # LS002007, Worthington Biochemical Corporation, Lakewood, NJ, USA). Samples with the cell viability >80 % and the cell concentration of 700–1200 cells/ μ L were selected to complete subsequent experiments. Subsequently, cleaning, re-suspension, and uploading of single-cell suspension samples were completed. After the formation of Gel Beads in Emulsions (GEMs), the samples were transferred to the Polymerase Chain Reaction (PCR) tubes. After reverse transcription and library construction, the 10x single-cell transcriptome library was constructed using an Illumina sequencer (Cat # novaseq6000, Illumina, San Diego, CA, USA).

Data Analysis Process

The preprocessed gene expression matrix generated by the Cell Ranger pipeline was imported into Seurat (v.4.3.0) (Stuart *et al.*, 2019) for downstream analysis. During quality control, genes expressed in fewer than three cells were removed, and cells were filtered based on detected gene numbers, UMI counts, and mitochondrial gene expression, with thresholds set at 1000–20,000 for UMI counts, 200–5000 for detected genes, and less than 20 % for mitochondrial gene expression. The filtered gene expression matrix was normalized using the “NormalizeData” function with default parameters (normalization. Method = “LogNormalize”, scale.factor = 10,000), followed by scaling and regression with “ScaleData” to remove the effects of UMI count variations and mitochondrial content percentages. Principal component analysis (PCA) was performed on the scaled data, restricted to the top 2000 variable genes identified by “FindVariableFeatures” with default settings, and different samples were integrated using the “Harmony” package (v1.0) with the top 20 principal components as input for the “RunHarmony” function. Cell clusters were identified using the “FindClusters” function at a resolution of 0.5, and major cell types were annotated with “SingleR” (Aran *et al.*, 2019). Subsequently, we performed subcluster identification using the FindSubCluster function. The annotation of these subclustered cells primarily relied on previously curated canonical marker genes.

The FindMarkers function was then used to identify differentially expressed genes (DEGs) between different cell clusters, employing the Wilcoxon rank-sum test as the statistical method, with a false discovery rate (FDR) threshold set at <0.05 to identify significant candidate genes. To explore intercellular communication among different cell clusters, the CellChat package was utilized (Jin *et al.*, 2021). We constructed cell-cell communication networks for each cell type, assessing the strength and importance of ligand-receptor interactions. Using CellChat, we quantified the changes in communication pathways between different cell types and visualized these interactions using heatmaps and bubble plots. For investigating cell differentiation trajectories and potential developmental paths, the monocle package was applied. Dimensionality reduction was per-

formed on the gene expression data using the DDRTree method to identify pseudotime trajectories, allowing us to infer dynamic transitions between different cell states and identify dynamic expression patterns of key genes during differentiation. To gain deeper insights into the biological functions of differentially expressed genes, gene functional enrichment analysis was conducted using the clusterProfiler package (Yu *et al.*, 2012). Gene Set Enrichment Analysis (GSEA) was carried out employing gene sets provided by scMetabolism (Wu *et al.*, 2022) and GSEABase to identify significantly enriched KEGG pathways and GO biological processes in different cell clusters, with a significance threshold of $p.adjust < 0.05$ to explore relevant biological functional modules. All data processing and visualization were performed within the R programming environment, with analysis results presented through various graphical representations, including violin plots, heatmaps, bubble plots, and trajectory plots, to display research findings in a clear and intuitive manner.

Multiple Immunofluorescence Staining

Three normal and degenerated meniscus specimens of varying severity obtained from human knee arthroplasties were fixed in 4 % paraformaldehyde, embedded in paraffin, and sliced. Serial staining was performed with the TSAPlus Fluorescent Staining Kit (Cat # G1257-50T, Servicebio, Wuhan, China). Ch.1 (SERPINA1), Ch.2 (MMP14), Ch.3 (CDON), Immune cell (CD45), endothelial cells (*VWF*), Macrophage (CD163), and PCL (*ACTA2*) were labeled simultaneously on the same tissue section using different primary antibodies. The images were acquired using Panoramic MIDI scanner (Cat # 5076, 3DHISTECH, Budapest, Hungary). And the false color was set to distinguish. The primary antibodies for incubating specimens include SERPINA1 (Cat # A21972, 1:1000, ABclonal, Woburn, MA, USA), MMP14 (Cat # A2549, 1:1000, ABclonal, Woburn, MA, USA), CDON (Cat # sc-377232, 1:500, Santa Cruz Biotechnology, Dallas, TX, USA), CD45 (Cat # GB14038-50, 1:1000, Servicebio, Wuhan, China), *VWF* (Cat # GB11020-100, 1:1000, Servicebio, Wuhan, China), CD163 (Cat # GB115709-100, 1:5000, Servicebio, Wuhan, China), *ACTA2* (Cat # GB12044-100, 1:5000, Servicebio, Wuhan, China) and IL1b (Cat # GB11113-100, 1:3000, Servicebio, Wuhan, China). Multicolor immunofluorescence staining utilizes the peroxidase reaction of tyramide based on tyramide signal amplification (TSA) technology to generate a series of enzymatic reactions that form a large number of fluorescein deposits at the antigen-antibody binding site to achieve signal amplification, and subsequently optimize the incubation sequence of the primary antibodies.

Proliferation and Apoptosis Staining

Three normal and degenerated meniscus specimens of varying severity obtained from human knee arthroplasties

were fixed in 4 % paraformaldehyde, embedded in paraffin, and sectioned. Cell proliferation was assessed using the Click-iT EdU-488 Cell Proliferation Detection Kit (Cat # G1601, Servicebio, Wuhan, China). The staining was performed according to the manufacturer's instructions. Briefly, the sections were incubated with EdU solution, followed by reaction with the Click-iT reaction cocktail to label proliferating cells. DAPI was used for counterstaining to visualize nuclei. Cell apoptosis was evaluated using the One-Step TUNEL Apoptosis Assay Kit (Cat # KGA1405-50, KeyGEN BioTECH, Nanjing, China). The staining was conducted as per the protocol provided by the manufacturer. The sections were incubated with the TUNEL reaction mixture, followed by DAPI counterstaining. Both EdU and TUNEL stained sections were scanned using a Panoramic MIDI scanner. The images were acquired and analyzed to determine the proliferation and apoptosis rates in the meniscus samples.

Results

scRNA-seq Revealed Different Cell Types in Synovium and Meniscus Samples

To identify the expression profiles of cells in the normal and degenerated synovium and meniscus samples, as shown in **Supplementary Fig. 2a**, a total of 124,026 cells from 22 samples of 16 knee osteoarthritis (KOA) patients were sequenced by scRNA-seq (Fig. 1a, **Supplementary Fig. 1** and **Supplementary Table 1**), including 35,635 synoviocytes (synovial lining fibroblasts, synovial sublining fibroblasts, *CXCL14*+ fibroblasts (*CXCL14*+ Fibs), fibroblast_1, and fibroblast_2), 38,936 meniscus cells (Ch.1, Ch.2, Ch.3, Ch.4, and Ch.5), 23,856 immune cells (B cells, T cells, dendritic cells (DCs), mast cells, macrophages (Macs)), 16,223 endothelial cells (capillary-venous and capillary-arterial), 9376 pericyte-like cells (PCL) (pericyte-like cells_1 and pericyte-like cells_2). These cells were divided into 24 separate clusters using the unsupervised clustering algorithm. The heterogeneity of cell types was significant (**Supplementary Fig. 1d** and **Supplementary Fig. 2c–e**). These cells were visualized through the uniform manifold approximation and projection (UMAP) and t-Distributed Stochastic Neighbor Embedding (tSNE) (Fig. 1c–e). The number of genes per cell and that of counts per cell, as well as the PCA of genes with large variations, are shown in **Supplementary Fig. 1a–c**. Except for the H12 inner samples from the public database, other samples were of good quality. The cell type was identified by markers in Fig. 1f, **Supplementary Fig. 2b** and **Supplementary Figs. 3,4**. The cell clusters with high expression of cartilage-related genes were renamed chondrocytes, such as *CHAD*, *PRG4*, *TGF-β1*, *CDF*, *STMN1*, *COL3A1*, *DCN*, and *LUM*. Additionally, 5 kinds of meniscus fibroblasts were defined as per Fu *et al.* (2022), including Ch.1 (*CHAD*+), Ch.2 (*FNDC1*+), Ch.3 (*PRG4*+), Ch.4 (*CFD*+), and Ch.5 (*STMN1*+ (**Supplementary Fig. 5a**).

The cells with high expression of *VWF* and *PECAM1* were identified as endothelial cells, including endothelial cell (capillary-venous) (ECs (CAP-V)) (*GJA5*+), and endothelial cell (capillary-arterial) (ECs (CAP-A)) (*VWF*+). The smooth muscle cells and mural cells with high expression of *ACTA2*, *MYL9*, and *TAGLN* were named pericyte-like cells, PCL.1 (*ACTA2*+ and *FABP4*+), and PCL.2 (*ACTA2*+ and *MYH11*+ (**Supplementary Fig. 5b,c**). As defined in previous articles, there were 3 kinds of fibroblasts, including synovial lining fibroblasts (SIFs), synovial sublining fibroblasts (SSFs) (Wei *et al.*, 2020; Zhang *et al.*, 2019), and *CXCL14*+ fibroblasts (*CXCL14*+ Fibs) (Micheroli *et al.*, 2022), 2 newly defined subtypes, including Fibroblast_1 (Fib_1) and Fibroblast_2 (Fib_2), and 1 transitional subtype, namely synovial fibrochondrocytes (FCs) (Ji *et al.*, 2019; Sun *et al.*, 2020). Moreover, *CD79A* and *CD27* were used to identify B cells, *CD2* and *CD8A* to identify T cells, *LYVE1*, *FOLR2*, and *MRC1* to identify macrophages (Macs), and *CD1C*, *CLEC10A*, and *FCGR2B* to identify dendritic cells (DCs).

scRNA-seq Revealed New Fibroblast Subtypes

The term “fibrochondrocytes” can be traced back to the 1984 study on fibrochondrogenesis by Whitley *et al.* (1984). In recent years, to prepare favorable meniscus repair materials, the focus of many studies has been placed on promoting the fibrocartilage differentiation of synovium-derived stem cells (Fox *et al.*, 2010; Qu *et al.*, 2019). In this process, investigators from several laboratories isolated fibrochondrocytes from meniscus cells (Gunja and Athanasiou, 2007). Among them, Ji *et al.* (2019) isolated fibrocartilage chondrocytes (FCs) from the cartilage with the aid of scRNA-seq for the first time. Besides, Sun *et al.* (2020) used a similar method to identify fibrochondrocytes (FCs) with high expression of *COL3A1*, *COL6A1*, and *COL1A1*. In short, these results indicated that the markers of this cell subtype included those of chondrocytes (such as *COL3A1* and *COL6A*) (Sun *et al.*, 2020) and synovial fibroblasts (such as *PRG4*) (Wei *et al.*, 2020). Hence, it can be maintained that this is a transitional subtype and may exist in synovium and meniscus samples. Similar to previous studies, it was found that this cell subtype can highly express the markers of chondrocytes and synovial fibroblasts, among which *BGN*, *COL6A1*, and *COL3A1* were the markers of Ch.2 (Fu *et al.*, 2022), and *HTRA1* and *PRG4* were the markers of SIFs (Wei *et al.*, 2020; Zhang *et al.*, 2019). FCs were found in meniscus and synovium samples (Fig. 1b), with a larger number in meniscus samples. The pseudotime analysis was performed in synovium and meniscus samples, respectively. It can be observed that FCs were mainly distributed around the starting point of the trajectory in synovium samples and the trajectory's root of the pseudotime trajectory in meniscus samples. In the clustering process, two newly defined subtypes, Fibroblast_1 (Fib_1) and Fibroblast_2 (Fib_2), were observed. Both subtypes can ex-

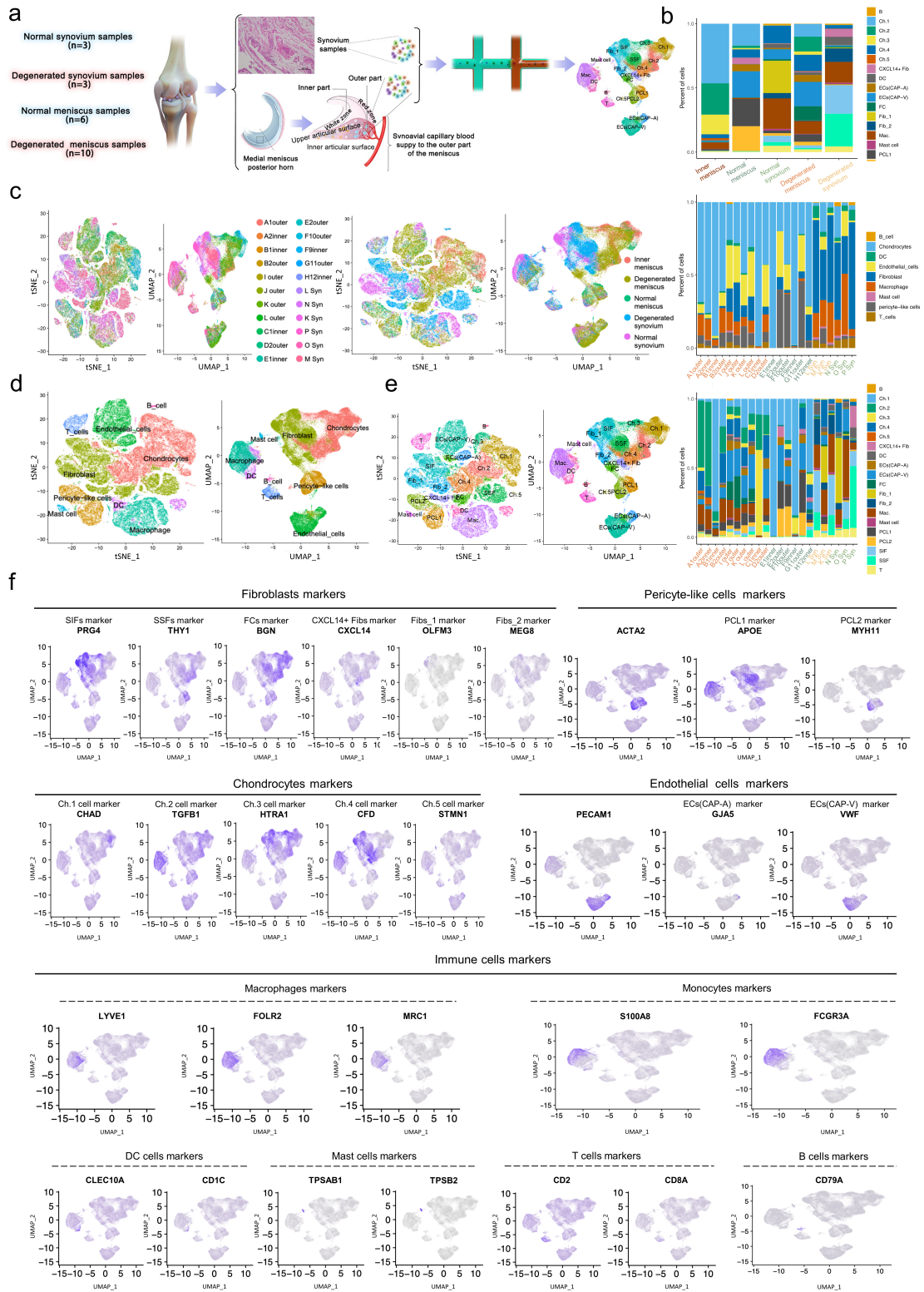


Fig. 1. Single-cell RNA sequencing (scRNA-seq) revealed the main cell types in synovium and meniscus samples. (a) The overall workflow of scRNA-seq. Synovium/meniscus samples were collected from non-osteoarthritis (OA) and OA patients. Some samples were collected from the online database The Genome Sequence Archive for Human (GSA-Human) PRJCA008120. **(b)** The proportion of cell subsets in the degenerated and normal meniscus and synovium samples. **(c)** Visualization of all meniscus/synovium samples through t-Distributed Stochastic Neighbor Embedding (tSNE) and uniform manifold approximation and projection (UMAP) with donor origins. **(d)** Visualization of cell identity compartments of all meniscus/synovium samples through tSNE and UMAP. **(e)** Visualization of main cell types through tSNE and UMAP. **(f)** The expression level of marker of main cell subtypes.

press the marker (*PRG4*) of synovial fibroblasts, mainly in synovium samples (Fig. 1b). Fib_1 was mainly observed in the normal synovium samples, while Fib_2 was mainly observed in degenerated synovium samples (Fig. 1b).

The CellChat-Based Analysis Revealed the Changes in Synovium/Meniscus Samples Caused by the Progression of OA

The crosstalk was observed in normal and degenerated meniscus and synovium samples based on CellChat. Of note, the interaction between over-expressed ligands and receptors in meniscus chondrocytes and synovial fibroblasts can be observed in different tissue samples. A variety of cells were found to have extensive correlations in the internal environment of KOA. It was observed that there were several different expression patterns in normal and degenerated meniscus and synovium cells. The inflammation-related pathways critical to the progression of OA were up-regulated in degenerated samples compared with normal samples, including the insulin-like growth factor (IGF) (Busby Jr *et al.*, 2009), pleiotrophin (*PTN*) (Zhu *et al.*, 2021), and fibroblast growth factor (FGF) pathways in OA and the Midkine (MK) pathway in rheumatoid arthritis (RA) (Maruyama *et al.*, 2004). Besides, the cartilage regulatory pathways (such as angiopoietin-like protein (ANGPTL), protein S (PROS), and platelet-derived growth factor (PDGF) pathways) and vascular regulatory pathways (such as VISFATIN (Liao *et al.*, 2016), vascular endothelial growth factor (VEGF) (Hamilton *et al.*, 2016), and semaphorin 3 (SEMA3) (Okubo *et al.*, 2011) pathways) were up-regulated in degenerated samples. On the contrary, the GALECTIN pathway (Toegel *et al.*, 2016; Weinmann *et al.*, 2016), CXCL pathway, transforming growth factor beta (TGF- β) pathway (Fernandes *et al.*, 2020), and other pathways related to macrophage polarization were down-regulated in degenerated samples.

Based on that, it can be assumed that the meniscus and synovium may exhibit similar CellChat trends during the development of OA. The CellChat-based analysis of normal and degenerated meniscus and synovium samples may provide a new method for understanding the synergistic effects from the mechanisms related to OA progression between tissues (meniscus and synovium) and cells (chondrocytes and fibroblasts). Subsequently, a CellChat-based analysis was performed to explore the interaction between synovial fibroblasts and chondrocytes.

The Crosstalk between Synovium and Meniscus in Key Pathways in OA

The IGF pathway, *PTN* pathway, MK pathway, and FGF pathway were highly expressed in OA samples (Busby Jr *et al.*, 2009; Maruyama *et al.*, 2004; Zhu *et al.*, 2021). In the progression of OA, 4 pathways presented extremely similar trends in meniscus and synovium samples. Significant crosstalk between synovial fibroblasts and chon-

drocytes can be observed in normal and degenerated samples (Fig. 2 and **Supplementary Fig. 6a**). In particular, there were more and stronger interactions between SSF (senders) and Ch.1–5 (receivers) in degenerated samples than in normal samples. This was consistent with previous findings, namely that insulin-like growth factor 1 (*IGF-1*) and pleiotrophin (*PTN*) were highly expressed in the OA cartilage (Martel-Pelletier *et al.*, 1998; Morales, 2008; Pufe *et al.*, 2003). Besides, fibroblast growth factor-18 (*FGF-18*), a key molecule in the FGF signaling pathway, was highly expressed in the OA synovium (Takata *et al.*, 2021). This may be related to the expression of MMP-13 in chondrocytes induced by *bFGFs* (Im *et al.*, 2009). Of note, there is no research on the role of the MK pathway (a pathogenic pathway related to RA) in OA, and there is no report with a focus on the expression patterns of the above 4 pathways in the OA synovium. These results suggested that synovial fibroblasts (senders) were involved in the changes of multiple pathways during the degeneration of tissues. The whole Cellchat pattern in different samples was further observed. It was found that synovium samples presented more active communication patterns, and normal synovial tissues also exhibited complex communication patterns. This also verified that the occurrence of OA may be earlier than that of cartilage inflammation, suggesting the significance of early intervention in the management of synovitis (**Supplementary Fig. 6b**).

The Crosstalk between Synovium and Meniscus in Cartilage Regulatory Pathways

It can be observed that the ANGPTL pathway, PDGF pathway, and PROS pathway presented similar trends in the CellChat-based analysis during the progression of OA. Ch.1–5, SSF, and SIF (senders) had more interaction and stronger interactions in degenerated samples (**Supplementary Figs. 7,8**). This phenomenon was more prominent in meniscus samples. This may be related to 3 pathways that can lead to disease progression by affecting the growth of articular cartilage or cartilage vessels (Gerwin *et al.*, 2022; Su *et al.*, 2020; Suleiman *et al.*, 2013). From the observation of 3 pathogenic pathways in degenerated samples: SIF and SSF (senders) exhibited a larger communication probability than Ch.1–5 (senders). This suggested that synovial fibroblasts may play an important role during the degeneration of tissues. In normal meniscus samples, it can only be observed that *PRG4*+ Ch.3 (senders) ligands acted on various cell receptors. Of note, this special chondrocyte subtype was distributed on the meniscus surface and can highly express *PRG4*, an *HTRAI* marker gene, which was common in the synovium (Fu *et al.*, 2022). These results verified that the synovium may play a role in the progression of OA (de Lange-Brokaar *et al.*, 2012).

Normal meniscus vs. Degenerated meniscus vs. Normal synovium vs. Degenerated synovium

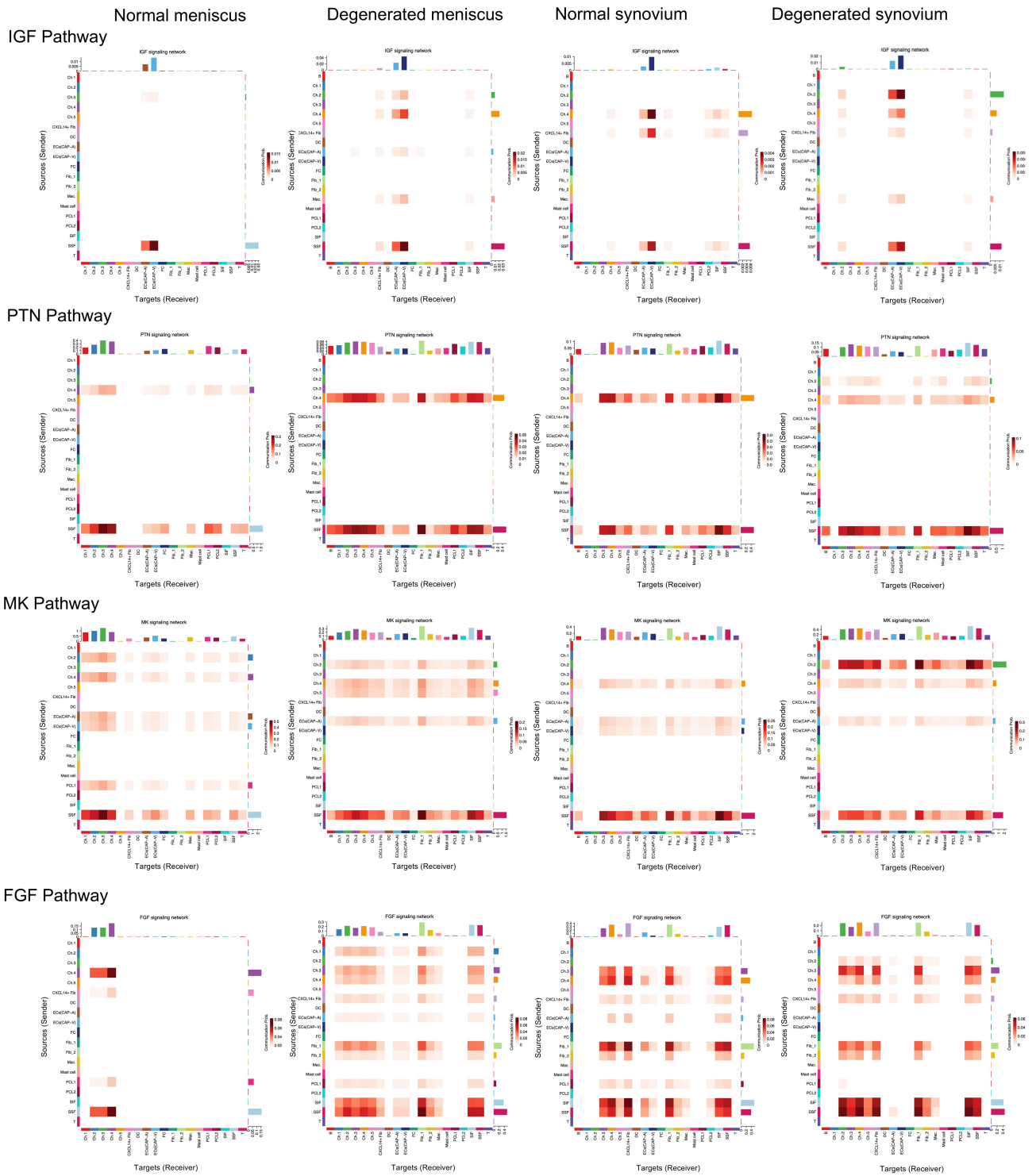


Fig. 2. Cellular communication revealed by OA-related pathway through CellChat. The heatmap (based on CellChat analysis) revealed the interaction numbers and communication probabilities in cellular communication networks among the normal meniscus, degenerated meniscus, normal synovium, and degenerated synovium groups.

The Crosstalk between Synovium and Meniscus in Neovascularization Pathways

ECs (CAP-A) and ECs (CAP-V) (receivers) exhibited a larger communication probability in the VISFATIN pathway, VEGF pathway, and SEMA3 pathway, presenting similar trends in the CellChat-based analysis (**Supplementary Figs. 9,10**). Besides, there were more interactions between ECs (receivers) in the degenerated group than in the normal group in meniscus samples. These results were consistent with previous findings, namely that the VISFATIN pathway (Liao *et al.*, 2016; Tsai *et al.*, 2020), VEGF pathway (Hamilton *et al.*, 2016; Murata *et al.*, 2008), and SEMA3 pathway (Okubo *et al.*, 2011) promoted the progression of OA by regulating neovascularization during cartilage development. VISFATIN up-regulated the expression of vascular endothelial growth factors (VEGFs) in human OA synovial fibroblasts and promoted tube formation and migration of endothelial progenitor cells (Tsai *et al.*, 2020). VEGF was highly expressed in the OA cartilage (Enomoto *et al.*, 2003) and involved in angiogenesis and chondrocyte metabolism (Murata *et al.*, 2008), thus promoting the expression of MMPs in chondrocytes (Pufe *et al.*, 2004).

Besides, significant communication between macrophages (senders) and ECs (receivers) can be observed in synovium samples. This was consistent with previous findings, namely that VEGF secreted by macrophages can promote angiogenesis and aggravate inflammation in the OA synovium (Haywood *et al.*, 2003). It was also found that ECs (receivers) in degenerated meniscus samples exhibited a larger communication probability than those in normal meniscus samples. This may be attributed to the binding of *SEMA3A* to neuropilin 1 (NRP-1), which served as an antagonist of VEGF signaling transduction in ECs (Okubo *et al.*, 2011). These results were similar to those of Enomoto *et al.* (2003) in that the VEGF receptor neuropilin 1 (NRP-1) was up-regulated in the OA cartilage. In addition, *SEMA3A* was highly expressed in chondrocytes of the OA meniscus. This may be related to the inhibitory effect of semaphorin 3A (*SEMA3A*) on the protective migration of VEGF165 in chondrocytes reported by Okubo *et al.* (2011). In this study, it was also found that the communication probability of meniscus chondrocytes (receivers) in degenerated meniscus samples was larger than that in normal meniscus samples. Moreover, the above 3 pathways presented similar trends in the interaction number and strength in degenerated meniscus, normal synovium, and degenerated synovium samples. This may be related to the angiogenesis of synovial tissues and cartilage tissues during the progression of OA (Smith *et al.*, 1997). Additionally, the early high expression of pathway ligand molecules in the synovium may act on meniscus tissues through the synovial fluid (Blom *et al.*, 2007). In summary, these results validated the views of other researchers (Sanchez-Lopez *et al.*, 2022).

Vascular regulatory signaling pathways may construct the communication between synovium and meniscus in the process of degeneration.

The Crosstalk between Synovium and Meniscus in Macrophage Polarization Pathways

The GALECTIN pathway (MacKinnon *et al.*, 2008), CXCL pathway (Unver *et al.*, 2015), and TGF- β pathway (Fernandes *et al.*, 2020) (some pathways related to macrophage polarization) presented similar trends in the CellChat-based analysis (**Supplementary Figs. 11,12**). Fernandes *et al.* (2020) also found that monocytes (M) 2 polarization of macrophages can promote the repair of cartilage and synovium (Sanchez-Lopez *et al.*, 2022). The GALECTIN pathway (Toegel *et al.*, 2016; Weinmann *et al.*, 2016) of chondrocytes (receivers), a harmful upstream mediator of the cartilage, presented significant differences in the interaction of meniscus samples. This may be related to the role of GALECTIN-1 as an upstream mediator of inflammation and matrix decomposition in OA. The secretion of GALECTIN-1 was not induced by proinflammatory conditions (Toegel *et al.*, 2016; Weinmann *et al.*, 2016). This may be attributed to the high GALECTIN pathway activity in normal meniscus samples. GALECTIN-3 can drive M2 polarization of macrophages in mice (MacKinnon *et al.*, 2008). This also suggested that the GALECTIN pathway was involved in macrophage-related mechanisms. In particular, the strength of interactions between the antigen-presenting cells (APCs) (senders) of macrophages/DCs and the GALECTIN pathway of DCs (receivers) in degenerated synovium and meniscus samples was weakened compared with normal samples. Moreover, the CXCL pathway between APCs (senders) and ECs (CAP-V) (receivers) decreased in degenerated samples of different tissues.

There are many experiments with a focus on the angiogenesis of the CXCL pathway (Bernardini *et al.*, 2003; Wu *et al.*, 2012). The serum level of CXCL8, CXCL9, CCL2, and CXCL10 in patients with KOA increased with age (Bonfante *et al.*, 2017). CXCL7 can promote M2 polarization of macrophages in tumors (Sica and Mantovani, 2012). M1 and M2 polarization of macrophages can secrete different CXCL molecules (Mosser, 2003). It can be assumed that the crosstalk between APCs (senders) and ECs (receivers) may be involved in the regulation of macrophage polarization through the CXCL pathway. The communication probability between macrophages (senders) and Ch2 and Ch5 (receivers) decreased in synovium samples. Changes in the anti-inflammatory and pro-chondrogenic cytokine transforming growth factor- β (TGF- β) secreted by macrophages with disease progression can also be observed. The increased secretion of TGF- β in M2 macrophages contributed to the repair of cartilage by MSCs (Fernandes *et al.*, 2020). The decreased secretion of TGF- β may be the common initiating factor for meniscus and synovial metamorphosis. Macrophage (senders) pre-

sented similar trends in the GALECTIN pathway, CXCL pathway, and TGF- β pathway between different samples. Macrophages played an important role in the whole progression of OA. However, it remains undefined that macrophage infiltration mainly affects the early stage (Benito *et al.*, 2005) or the end stage (Roemer *et al.*, 2010). In summary, these results suggested that the pathways related to macrophage polarization had similar action patterns in synovium and meniscus samples. Crosstalk between the inner meniscus samples and the degenerated meniscus samples is shown in **Supplementary Fig. 13**.

Analysis of the Dynamic Relationships between Synovial Fibroblast and Meniscus Chondrocyte Subtypes

A total of 11 subtypes were selected to construct a new trajectory, including 6 synovial fibroblasts (SIFs, SSFs, CXCL14+ Fibs, Fib_1, Fib_2, and FCs) and 5 meniscus chondrocytes (Ch.1, Ch.2, Ch.3, Ch.4, and Ch.5). In synovium samples, the trajectory root was mainly populated by FCs, while the two primary termini of the tree were populated by Ch.2 and Fib_2 of cell fate 1 and Ch.3, Ch.5, and Fib_1 of cell fate 2 (Fig. 3a,b). In meniscus samples, cell fate 1 was populated by FCs and Fib_2, and cell fate 2 was populated by SSFs (Fig. 3b,c). Several genes that changed significantly during the transformation were identified in the pseudotime differential expression analysis. Fig. 3d,e presents the genes with the most significant changes in the pseudotime trajectory in the heatmap. In the synovium pseudotime heatmap, cluster 4 was populated by Ch.4 (*EFEMP1* and *CFH*), Ch.3 (*PRELP*), and Ch.1 (*CHI3L2* and *CHI3L1*), and its expression was down-regulated with the progression of OA. In cluster 3, marker genes (*CD55* and *PRG4*) of SIFs were highly expressed with the progression of OA, and the number of SIFs in degenerated synovium samples was significantly higher compared with normal synovium samples (Fig. 1b). It can be speculated that SIFs played an important role in degenerated synovium samples. Additionally, SSFs, SIFs, CXCL14+ Fib, and Fib_2 were exclusively present in the pseudotime trajectory of degenerated synovium samples, while Fib_1 predominantly occupied the pseudotime trajectory of normal synovium samples. Notably, Fib_1 was primarily associated with synovium cell fate 2, in contrast to SSFs, SIFs, and CXCL14+ Fib, which were associated with synovium cell fate 1. These findings suggest that synovium cell fate 2 may represent a normal cell state during degeneration, characterized by conservative cellular development that may play a role in inhibiting inflammatory progression. In contrast, cell fate 1 may indicate an abnormal cell state in degenerated specimens.

In meniscus samples, the expression of genes of clusters 2 and 3 was up-regulated, and that of cluster 4 was down-regulated with the progression of OA. Of note, the marker genes of Ch.2 (*COL6A3*), Ch.3 (*COL3A1*, *FNI*, and *TNFAIP6*), and Ch.4 (*PLA2G2A*, *EFEMP1*, and *CYP11B1*)

in clusters 2 and 3 were highly expressed with the progression of OA; while, the marker genes of Ch.1 (*FGFBP2*, *APOD*, *CYR61*, *C2orf40*, *CHI3L2*, *CHI3L1*, and *CP*) exhibited a reverse expression trend. Overall, Ch.1–5 chondrocytes predominantly occupied the pseudotime trajectory in meniscus samples, forming the trajectory root in normal meniscus and the termini of two cell fates in degenerated meniscus samples (Fig. 3b). With the progression of OA, the expression of marker genes of Ch.2–5 was up-regulated significantly; while the expression of marker genes of Ch.1 was down-regulated. This result verified the finding of Fu *et al.* (2022), namely that Ch.1 may be a normal subtype and can maintain the homeostasis of meniscus tissues. Except for Ch.4, few chondrocytes could populate the pseudotime trajectory of synovium samples, which may be explained that Ch.4 had the markers of SSFs such as *CXCL12* (Fu *et al.*, 2022). The fibroblasts/chondrocyte intermediate subtype FCs populated the root of synovium samples and cell fate 1 of meniscus samples. The marker gene *COL3A1* of FCs was down-regulated in cluster 4 of synovium samples and up-regulated in cluster 2 of meniscus samples. This validated the hypothesis that the synergistic effect of synovium and meniscus was the initial factor in the progression of OA. FCs may play a role in this process.

Multiple Mechanisms Triggered the Progression of OA in Synovial Tissues

The Gene Set Enrichment Analysis (GSEA) results demonstrated that EPITHELIAL MESENCHYMAL TRANSITION (EMT), TNFA SIGNALING VIA NFKB, and other pathways exhibited common expression characteristics in various cells (Ch.3, Ch.4, Ch.5, Fib_2, DCs, ECs, PCL_1, and PCL_2). These gene sets related to inflammatory injury were highly expressed in normal synovium samples than in normal meniscus samples. In contrast, the expression of these gene sets was higher in degenerated meniscus samples than in degenerated synovium samples (Fig. 4a,b, **Supplementary Fig. 14a**). Synovium and meniscus samples can be considered as a whole, and hence the influence of the progression of OA on major joint tissues was analyzed as a whole. In most cells (Ch.1, Ch.3, Ch.4, Ch.5, Fib_1, Fib_2, FCs, ECs, mast cells, T cells, and DCs), the EMT and TNFA pathways were highly expressed in degenerated samples compared with normal samples (Fig. 4a,b, **Supplementary Fig. 14a**). Based on that, it was speculated that there was an inflammatory mechanism in the synovial and meniscus tissues that transferred from synovial tissues to meniscus ones, which could affect the degeneration of various tissues regarding bones and joints. Meanwhile, it was noticed that similar phenomena widely appeared in hypoxia and apoptosis (**Supplementary Fig. 15a,b**).

SIFs constituted an important cell subtype in the degenerated synovium. Different from the initial effects of degeneration of synovial tissues for most cells, SIFs exhibit

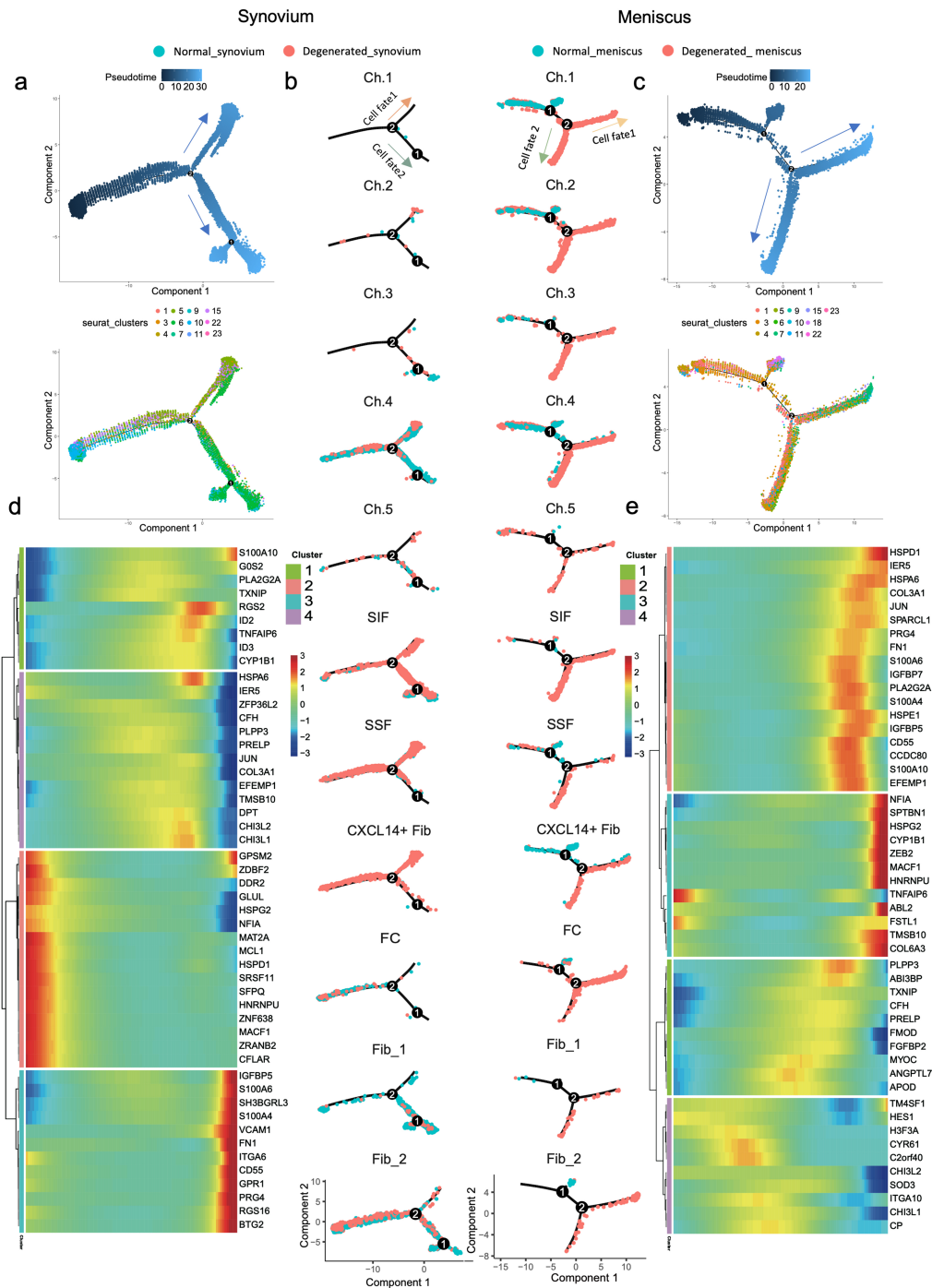


Fig. 3. Pseudotime analysis of synovial fibroblast and meniscus Chondrocyte subsets. (a) Monocle pseudotime trajectory showing the progression of synovial fibroblasts and meniscus chondrocytes in synovium samples. (b) Pseudotime trajectory of the progression of 11 kinds of synovial fibroblasts and meniscus chondrocytes. (c) Monocle pseudotime trajectory showing the progression of synovial fibroblasts and meniscus chondrocytes in meniscus samples. (d) The kinetic curve along the trajectory from the root to fate 1 and fate 2 presented from the left to the right of the heatmap. Ch.1 with the maker of *CHI3L2* and *CHI3L1*. Ch.3 with the maker of *PRELP*. Ch.4 with the maker of *EFEMP1* and *CFH*. Synovial lining fibroblasts (SIFs) with the maker of *CD55* and *PRG4*. (e) The kinetic curve from the root along the trajectory to the end presented from the left to the right of the heatmap. Ch.1 with the marker of *FGFBP2*, *APOD*, *CYR61*, *C2orf40*, *CHI3L2*, *CHI3L1*, and *CP*. Ch.2 with the marker of *COL6A3*. Ch.3 with the marker of *COL3A1*, *FN1*, *TNFAIP6*, and *PRELP*. Ch.4 with the marker of *PLA2G2A*, *EFEMP1*, *CYP1B1*, and *CFH*.



Fig. 4. The EPITHELIAL MESENCHYMAL TRANSITION (EMT) pathway played an important role in the synovium in the early stage of OA. (a) Differential expression of the HALLMARK EPITHELIAL MESENCHYMAL TRANSITION gene set in synovial fibroblasts and meniscus chondrocytes identified by Gene Set Enrichment Analysis (GSEA), with metabolic activity quantified by scMetabolism. (b) Similar analysis in inflammatory vascular-associated cells.

high expression of TNF, hypoxia, and other injury mechanisms in normal samples (Fig. 5a). Besides, these cells may participate in the mechanism initially inducing meniscus injury (Fig. 5b). Additionally, in the degenerated samples, the Ch.2 and *CXCL14*+ Fib cell populations showed low expression of genes associated with EMT, apoptosis, TNF α , hypoxia, and TNF α signaling via the NF- κ B pathway, all of which are typically involved in inflammatory injury responses in degenerated samples. Conversely, these cells displayed high expression of potential anti-inflammatory pathways, such as the mTORC pathway (Fig. 5c, **Supplementary Fig. 14b**, and **Supplementary Fig. 16a, b**). These findings suggest that SIFs, Ch.2, and *CXCL14*+ Fib may play a protective role in the meniscus and synovium of degenerated samples, consistent with previous studies (Fu *et al.*, 2022). Ch.2 (*FNDC1*) is a chondrocyte population associated with abnormal ECM degradation and remodeling.

Finally, the newly identified synovial fibroblast subtypes Fib_1 and Fib_2 were analyzed, respectively. In degenerated samples, both subtypes showed high expression of the TNFA and EMT pathways and low expression of HALLMARK INTERFERON GAMMA RESPONSE pathway (Fig. 4b, **Supplementary Fig. 17a**). The EMT pathway showed an upward trend in normal synovium samples and degenerated meniscus samples (**Supplementary Fig. 17b**). It can be speculated that the mechanism related to the progression of OA was limited to the synovium and other single tissues to a certain extent. Furthermore, EMT and other mechanisms can act on different tissues in the progression of OA at different stages. Compared with meniscus samples, the TNFA pathway in Fib_2 was highly expressed in normal and degenerated synovium samples (**Supplementary Fig. 17b**). This may be explained by the fact that Fib_2 is the main fibroblast subtype in degenerated synovium samples, while Fib_1 is the predominant subtype in normal synovium samples.

Distinguishing Cell Subtype Distribution by Immunofluorescence

Immunofluorescence staining was used to verify the spatial distribution of subtype markers in three human meniscus specimens with different clinical symptoms and radiographic grading (Kellgren-Lawrence grading scale (KL) 0, 3, 4). SERPINA1, MMP14, CDON, CD45, *VWF*, CD163, *ACTA2* and IL1b were selected for staining. Normal (KL_0) and Degenerated (KL_3, KL_4) meniscus specimens were stained simultaneously with the following antibodies: anti-SERPINA1 against meniscus subtype Ch.1, anti-MMP14 against Ch.2, anti-CDON against Ch.3, CD45 against immune cells, *VWF* against endothelial cells, CD163 against macrophages, anti-*ACTA2* against PCL cells, and anti-IL1b embodying inflammatory factors. Similar to previous studies (Fu *et al.*, 2022), a mixed distribution of SERPINA1+ Ch.1 and MMP14+ Ch.2 within the

meniscus was observed. CDON+ Ch.3 chondrocytes were predominantly distributed on the upper and lower meniscus articular surfaces, and *ACTA2*+ PCL appeared around *VWF*-positive vascular endothelial cells. In the outer part of the meniscus, blood supply of synovial capillaries to the meniscus could be observed, and CD45+ immune cells and CD163+ macrophages were distributed around the capillaries, some of which expressed IL1b. However, no cells positive for these molecules were observed on the upper and lower meniscus articular surfaces due to the absence of capillaries. Compared with normal specimens, the number of MMP14+ chondrocytes on the upper and lower meniscus articular surfaces increased in the Degenerated group, and there were more capillaries in the junction area between outer meniscus margin and synovium in the degenerated group. In addition, IF showed that in the degenerated group, the number of *ACTA2*+ PCL decreased, the number of immune cells such as vascular endothelial cells and macrophages increased, and the number of IL1b positive cells increased. IL1b was also significantly highly expressed on the upper meniscus articular surface of KL_4 (Fig. 6a,b, Fig. 7a).

Analysis of Proliferation and Apoptosis During OA Progression

In the KL_3 stage, there was a significant increase in apoptotic cells in the outer region of the meniscus compared to the KL_0 stage. Additionally, apoptotic cells were observed on both the upper and lower articular worn surfaces of the meniscus in KL_3 stage specimens. Interestingly, in KL_4 stage specimens, apoptotic cells were primarily located within the meniscus rather than on the articular surfaces (Fig. 7b). Similarly, EdU-positive proliferating cells were only observed near the small blood vessels in the articular surface and the outer part of the meniscus at the KL_3 stage (**Supplementary Fig. 18**).

Discussion

Investigators involving basic research pay attention to the pathogenesis of synovium, meniscus, cartilage, and other tissues in OA, and they attempt to identify and verify new therapeutic targets in OA-related tissues. At present, however, common drugs used in clinical practice only include glucocorticoids to relieve joint pain and sodium hyaluronate to protect the articular cartilage. This separation between clinical application and basic research results may be related to the fact that only differentially expressed genes (DEGs) in a single tissue are highlighted in previous studies (Chou *et al.*, 2020; Sun *et al.*, 2020). The integrative analysis of synovium and meniscus tissues provides a novel insight into the pathogenesis of OA. In OA, mechanical and metabolic factors can lead to high vascularization of synovial tissues (Smith *et al.*, 1997). Meanwhile, the structural damage from synovitis in OA has received attention from some researchers (Maglaviceanu *et*



Fig. 5. SIF, Ch.2, CXCL14, and other cell subtypes may play a protective role. (a) GSEA and scMetabolism analyses showed that the SIF in normal tissues was enriched for HALLMARK TNFA SIGNALING VIA NFKB and HALLMARK HYPOXIA. (b) GSEA was used to describe the activation of HALLMARK TNFA SIGNALING VIA NFKB of SIF in normal and degenerated meniscus and synovium samples. (c) GSEA and scMetabolism analysis comparing degenerated samples and normal samples.

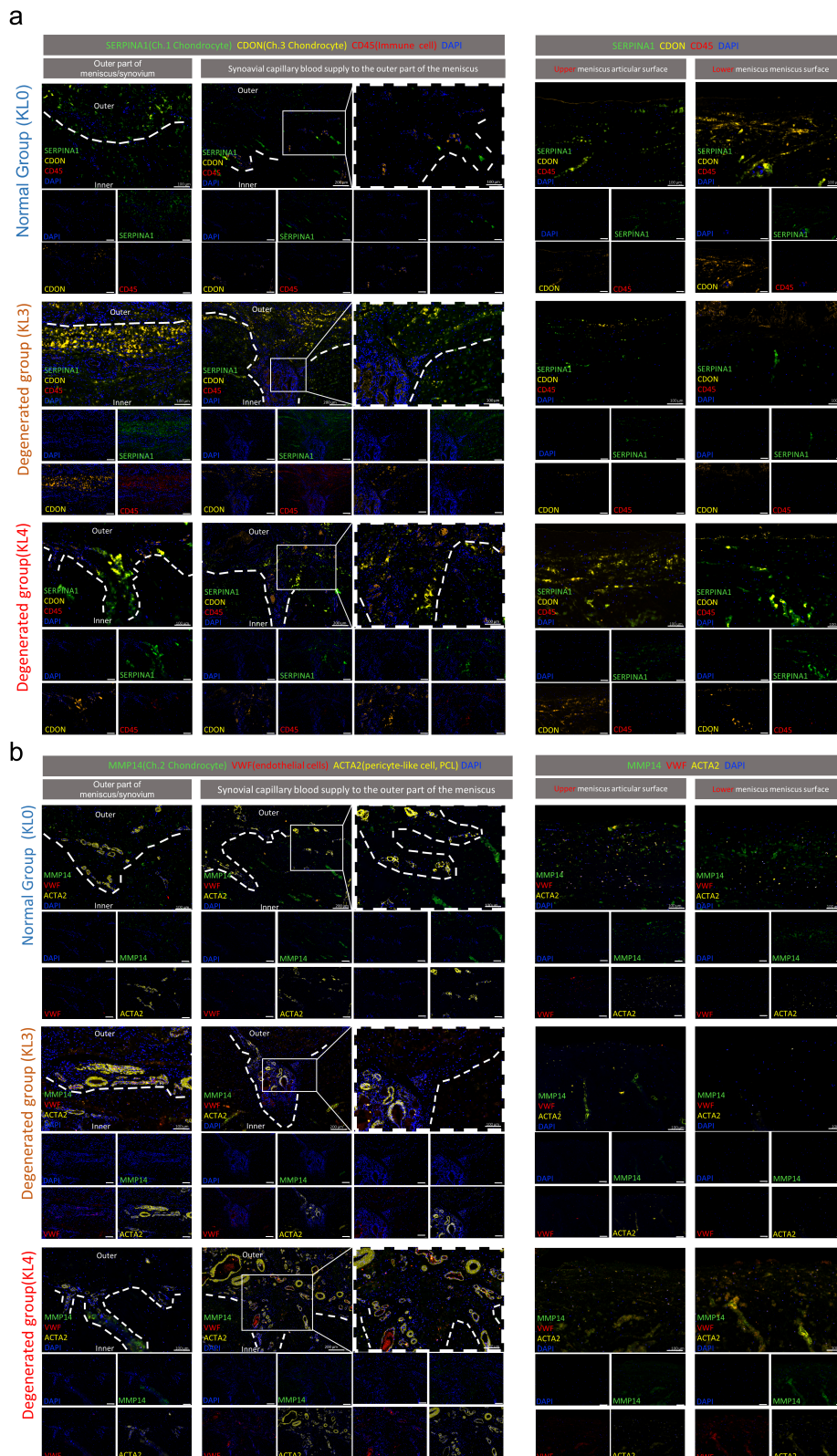


Fig. 6. Immunofluorescence staining of human meniscus showing intrinsic cell subtypes. The synovium/meniscus junction and upper and lower meniscus articular surfaces in the normal group and degenerated group were observed by IF staining. **(a)** Representative multicolor immunofluorescence staining image. Color settings: SERPINA1 for Ch.1 cells (green), CDON for Ch.3 cells (yellow), and CD45 for immune cells (magenta). Nuclei are stained blue (DAPI). **(b)** Color settings: MMP14 for Ch.2 cells (green), ACTA2 for pericyte-like cells (PCL) (yellow), and VWF for immune cells (magenta). Nuclei are stained blue (DAPI). IF, immunofluorescence.

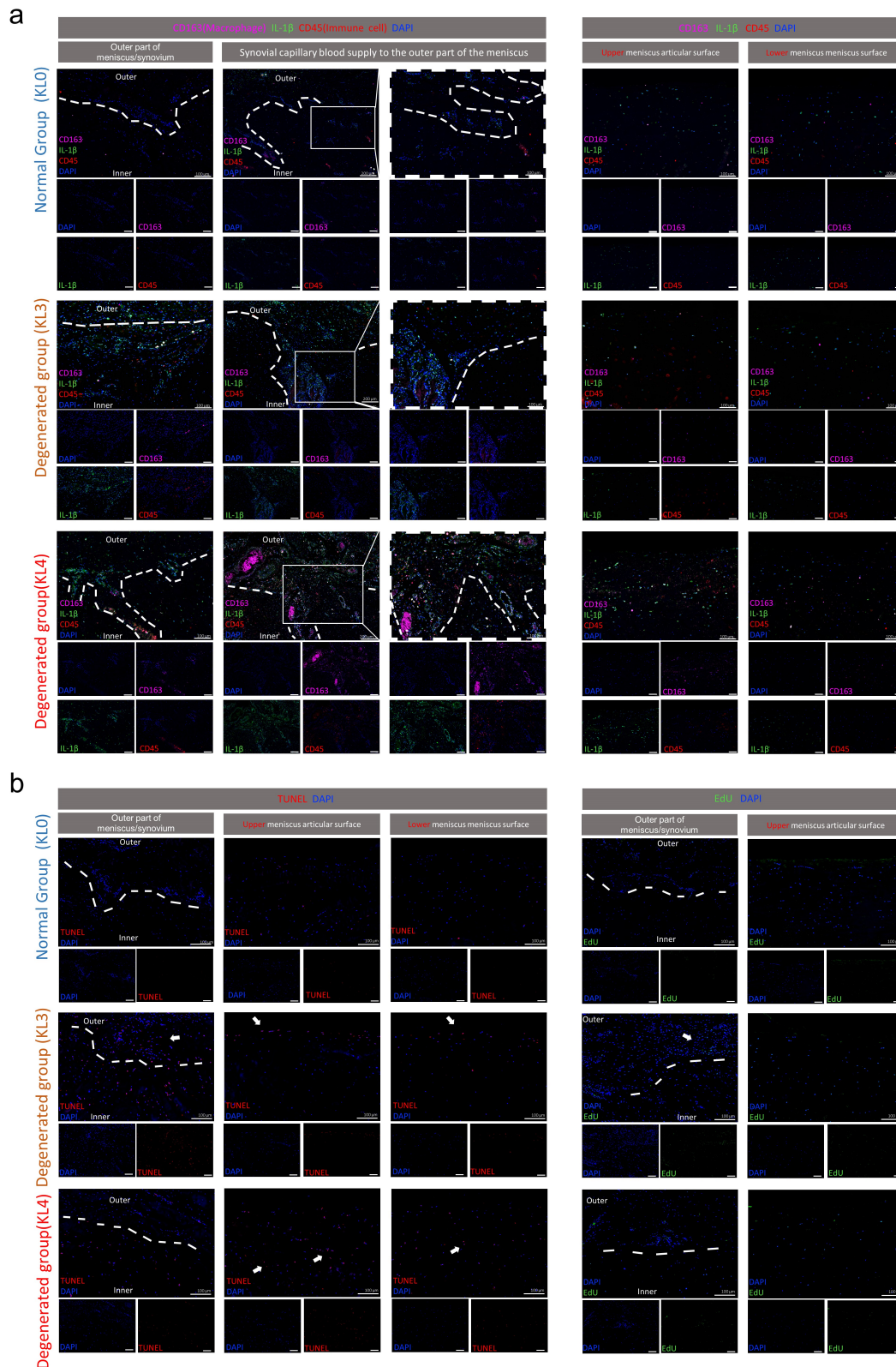


Fig. 7. Immunofluorescence Staining and Analysis of Proliferation and Apoptosis in Human Meniscus. (a) Immunofluorescence staining Color settings: IL-1 β (green), CD163 for Macrophage (Pink), and CD45 for immune cells (magenta). Nuclei are stained blue (DAPI). (b) The apoptosis and proliferation of cells in the normal group and degenerated group were observed using TUNEL staining and EdU staining.

et al., 2021). Synovium plays an important role in the occurrence and development of OA. Ultrasound (Sarmanova *et al.*, 2016), Magnetic Resonance Imaging (Atukorala *et al.*, 2016; Felson *et al.*, 2016), and other methods can be employed to verify the early pathogenesis of synovitis in OA (Smith *et al.*, 1997). Synovial lesions may precede and be related to cartilage injury. In contrast, the synergistic effect of synovium and meniscus in the progression of OA was only highlighted by Chou *et al.* (2020), who predicted the potential upstream regulatory factors of chondrocytes, thus inferring the cross-talk networks between cartilage and synovium tissues. However, synoviocytes and meniscus cells were not included in the same analysis system, and normal samples were also not taken into account. Therefore, the role of synovium/cartilage in the progression of OA cannot be evaluated.

In other disciplines, cancer cells with similar spatial positions but different tissue sources have been included in a single-cell analysis system (Li *et al.*, 2023). The cellular heterogeneity in cervical squamous cell carcinoma (SCC) and adenocarcinoma (AD) in similar microenvironments has also been collectively analyzed. This necessitates the overall consideration of transcriptome changes in different tissues in OA. Similar pathophysiological changes, fibroblast proliferation, neovascularization, and inflammatory cell infiltration can be observed during synovial and cartilage degeneration (Smith *et al.*, 1997).

In the multicolor immunofluorescence assay, more significant expression of inflammatory factors, capillary proliferation, and perivascular infiltration of myeloid cells were also observed in the degenerated group. Most studies have suggested that capillaries play a multifaceted role in the progression of OA (Fu *et al.*, 2022; Sun *et al.*, 2020), such as tissue repair and inflammatory progression in synovial and meniscal tissues. Changes in the number of endothelial cells and PCL cells were observed in the progression of OA, which may result in altered vascular permeability, and demonstrate a more complex crosstalk between meniscus and synovium in the degenerated group. Under physiological conditions, there was extensive communication between chondrocytes and synoviocytes (Li *et al.*, 2021b). The two kinds of cells can jointly promote the progression of inflammation in OA (Dreier *et al.*, 2001). Cytokines secreted by the inflammatory synovium (de Lange-Brokaar *et al.*, 2012) can act on cartilage tissues such as the meniscus and articular cartilage in the synovium fluid, and it may play a crucial role in the pathophysiology of OA (Steinhagen *et al.*, 2010). The potential mechanism of synovial injury mediating cartilage injury in OA in mice has been verified in a previous study (Blom *et al.*, 2007). Meanwhile, inflammatory cartilage can also promote the development of chronic synovitis (Hamasaki *et al.*, 2020; Silverstein *et al.*, 2017).

There are many studies with a focus on the associated pathways in synovium and meniscus samples (Chou *et al.*,

2020; Chau *et al.*, 2022). The FGF pathway was highly expressed in OA. Currently, many recombinant human fibroblast growth factor 18 (rhFGF18) drugs such as Sprifermin have entered phase II clinical trials and have been proved to exert anabolic effects on articular cartilage (Li *et al.*, 2021a). The angiopoietin-like proteins (ANGPTLs), a category of cartilage regulators, were expressed in cartilage differentiation (Gerwin *et al.*, 2022). In addition, ANGPTLs fulfilled functions in inflammatory tissue repair and participated in the progression of synovitis in OA (Nishiyama *et al.*, 2021). The performance of platelet-derived growth factors (PDGFs) in the CellChat-based analysis was consistent with that in previous studies (Su *et al.*, 2020). It was involved in the process that PDGFR- β secreted by PCL cells drove subchondral bone vessels to break through tidemarks and enter avascular cartilage (Su *et al.*, 2020). Recombinant protein S (PROS), a vitamin K-dependent plasma protein, played the role of cofactors of anticoagulant proteases. As a natural anticoagulant, protein S (PS) encoded by PROS has many potential biological functions (Suleiman *et al.*, 2013). It can be assumed that PS may promote the capillary formation in cartilage. The concentration of VISFATIN, VEGF, and SEMA3 in the serum of OA patients was higher than that in controls (Okubo *et al.*, 2011). They can promote vascular growth and maintain vascular networks, which could in turn stimulate the secretion of inflammatory cytokines (Tsai *et al.*, 2020). In the degenerated synovium and meniscus samples, T and B cells (senders) increased in the VISFATIN pathway and TGF- β pathway compared with normal samples, which was consistent with previous studies (Okubo *et al.*, 2011). Lymphocytes were rare in the synovium of patients with mild OA but more common in patients with severe OA (Smith *et al.*, 1997). GALECTIN-1, a key molecule in the GALECTIN pathway (a macrophage polarization pathway), was highly expressed in the degenerated cartilage of patients with severe OA, and it may induce inflammatory progression and matrix degradation. Different from the protective effect in RA, GALECTIN-1 promoted the progression of OA (Toegel *et al.*, 2016; Weinmann *et al.*, 2016). Besides, GALECTIN-1, GALECTIN-3, and GALECTIN-8 can synergistically promote the progression of OA (Weinmann *et al.*, 2018). Similar to the findings in previous studies, it was also found that mast cell and synovitis scores were positively correlated with the severity of OA (de Lange-Brokaar *et al.*, 2016). The TGF- β pathway between mast cells (senders) and chondrocytes and macrophages (receivers) can only be observed in degenerated samples.

The internal environment of the synovium, meniscus, cartilage, and synovial fluid in OA samples is characterized by cartilage regulation pathways, vascular regulation pathways, and macrophage polarization-related pathways. Our CellChat-based analysis of multiple pathways revealed that synovial fibroblasts (senders) play a significant role in the changes occurring in these pathways during

tissue degeneration. Key pathways, such as the IGF pathway, *PTN* pathway, MK pathway, and FGF pathway, which are highly expressed in OA, exhibited similar communication patterns. This similarity may reflect the histological homology between synovial and meniscal tissues, the resemblance of pathophysiological changes, and a synergistic mechanism throughout the degeneration process. Furthermore, the synergy and close relationship between synovial fibroblasts and chondrocytes are areas that merit further exploration. The CellChat-based analysis of the ANGPTL pathway, PDGF pathway, and PROS pathway underscored the important roles of synovial tissues and synovial fibroblasts. Additionally, the observations of the VISFATIN pathway, VEGF pathway, and SEMA3 pathway in the synovium and meniscus suggest the potential initiating effects of synovial fibroblasts.

To further observe this effect, we attempted to use TUNEL and EdU staining to track the most active regions of cell apoptosis and proliferation during the degenerative process. In the KL_3 meniscus-synovium junction tissue, we found a higher number of apoptotic cells, which might suggest the initiating role of synovial tissue in the early stages of OA. Interestingly, we only observed a small amount of EdU signal in KL_3 stage arthritis meniscus specimens. We speculate that this may reflect the abnormal capillary and chondrocyte proliferation in the inflammation-related outer part of the meniscus. In KL_4 stage specimens, apoptotic cells were observed only within the severely degenerative meniscus, which directly indicates meniscus damage in the late stages of OA. However, the initial role of synovium in early OA and its implications warrant further in-depth functional studies for validation.

Conclusions

To sum up, our results suggest a close crosstalk between the synovium and meniscus. The synovium may promote the progression of OA through its association with cartilage tissues and the crosstalk between synovial fibroblasts and meniscus chondrocytes. This descriptive study highlights the role of intra-articular tissues (synovium/meniscus) in this process. These findings provide a basis for understanding the cellular interactions involved in OA, which may inform future studies on early intervention in synovitis.

Our future research will focus on PCL cells present in both the synovium and meniscus. Although immunofluorescence experiments have observed a decrease in the number of *ACTA2*⁺ PCL cells during OA progression, this study did not observe communication between PCL cells and endothelial cells. Future studies on *ACTA2*⁺ PCL cells are expected to reduce vascular endothelial cell permeability in the synovium in OA, mitigating the pathological proliferation of synovial capillaries into the outer region of the meniscus. This may fundamentally reduce the complex crosstalk between the meniscus and synovium, thereby alle-

viating the spread of inflammation in intra-articular tissues in the early stages of OA and ultimately slowing down the degenerative changes in the knee joint.

List of Abbreviations

OA, osteoarthritis; KOA, knee osteoarthritis; scRNA-seq, single-cell RNA sequencing; GSA-Human, Genome Sequence Archive for Human; VEGF, vascular endothelial growth factor; SSCs, synovial mesenchymal stem cells; CPCs, chondrogenic progenitor cells; *PRG4*, proteoglycan 4; DEGs, differentially expressed genes; FCs, fibrochondrocytes; PCA, principal component analysis; FDR, false discovery rate; GSEA, Gene Set Enrichment Analysis; TSA, tyramide signal amplification; UMAP, uniform manifold approximation and projection; tSNE, t-Distributed Stochastic Neighbor Embedding; SIFs, synovial lining fibroblasts; SSFs, synovial sublining fibroblasts; *CXCL14*⁺ Fibs, *CXCL14*⁺ fibroblasts; Macs, macrophages; DCs, dendritic cells; EMT, EPITHELIAL MESENCHYMAL TRANSITION; MK, Midkine; IGF, insulin-like growth factor; FGF, fibroblast growth factor; ANGPTL, angiopoietin-like protein; PROS, protein S; PDGF, platelet-derived growth factor; SEMA3, semaphorin 3; *PTN*, pleiotrophin; *FGF-18*, fibroblast growth factor-18; NRP-1, neuropilin 1; APCs, antigen-presenting cells; TGF- β , transforming growth factor- β ; IF, immunofluorescence; SCC, squamous cell carcinoma; AD, adenocarcinoma; rhFGF18, recombinant human fibroblast growth factor 18; PS, protein S; KL, Kellgren-Lawrence grading scale; PCL, pericyte-like cells; ECs (CAP-V), endothelial cell (capillary-venous); ECs (CAP-A), endothelial cell (capillary-arterial); M, monocytes; Fib_1, Fibroblast_1; Fib_2, Fibroblast_2; *SEMA3A*, semaphorin 3A.

Availability of Data and Materials

The single-cell RNA sequencing raw data in Fastq format are available in the common storage library (The Genome Sequence Archive for Human (GSA-Human), <https://ngdc.cncb.ac.cn/gsa-human/>, with the login No. being HRA006091).

Author Contributions

FY, HZ, JW, and DLW contributed to the design of this work. TTQ analyzed the data. TBW, PL, YQC, and AX contributed to the interpretation of data. TTQ drafted the manuscript, and FY revised it critically for important intellectual content. All authors read and approved the final manuscript. All authors agreed to be accountable for all aspects of the work in ensuring that questions related to the accuracy or integrity of any part of the work were appropriately investigated and resolved.

Ethics Approval and Consent to Participate

The experiment was approved by the Biomedical Research Ethics Committee of Peking University Shenzhen Hospital (Approval No. 2019038). All patients have been informed of surgical excision costs. Tissue samples were collected, sequenced, and analyzed by the hospital sample bank. They agreed with the application of these tissues for this study and publication. All patients signed informed consent, and all authors have given their consent to participate.

Acknowledgments

Not applicable.

Funding

This research was supported by grants from National Natural Science Foundation of China (No. 82102568; No. 82172432), Shenzhen Key Medical Discipline Construction Fund (No. SZXK023), Shenzhen “San-Ming” Project of Medicine (No. SZSM202211038), Shenzhen Science and Technology Program (No. ZDSYS20220606100602005, No. JCYJ20220818102815033, No. KCXFZ20201221173411031, No. JCYJ20210324110214040, No. JCYJ20220531094406015), Guangdong Basic and Applied Basic Research Foundation (No. 2022A1515220111, No. 2022B1515120046, No. 2021A1515220054) and The Scientific Research Foundation of Peking University Shenzhen Hospital (No. KYQD2021099).

Conflict of Interest

The authors declare no conflict of interest.

Supplementary Material

Supplementary material associated with this article can be found, in the online version, at <https://doi.org/10.22203/eCM.v048a06>.

References

Aran D, Looney AP, Liu L, Wu E, Fong V, Hsu A, Chak S, Naikawadi RP, Wolters PJ, Abate AR, Butte AJ, Bhattacharya M (2019) Reference-based analysis of lung single-cell sequencing reveals a transitional profibrotic macrophage. *Nature Immunology* 20: 163-172. DOI: 10.1038/s41590-018-0276-y.

Atukorala I, Kwok CK, Guermazi A, Roemer FW, Boudreau RM, Hannon MJ, Hunter DJ (2016) Synovitis in knee osteoarthritis: a precursor of disease? *Annals of the Rheumatic Diseases* 75: 390-395. DOI: 10.1136/annrheumdis-2014-205894.

Benito MJ, Veale DJ, FitzGerald O, van den Berg WB, Bresnihan B (2005) Synovial tissue inflammation in early and late osteoarthritis. *Annals of the Rheumatic Diseases* 64: 1263-1267. DOI: 10.1136/ard.2004.025270.

Bernardini G, Ribatti D, Spinetti G, Morbidelli L, Ziche M, Santoni A, Capogrossi MC, Napolitano M (2003) Analysis of the role of chemokines in angiogenesis. *Journal of Immunological Methods* 273: 83-101. DOI: 10.1016/s0022-1759(02)00420-9.

Blom AB, van Lent PL, Libregts S, Holthuysen AE, van der Kraan PM, van Rooijen N, van den Berg WB (2007) Crucial role of macrophages in matrix metalloproteinase-mediated cartilage destruction during experimental osteoarthritis: involvement of matrix metalloproteinase 3. *Arthritis and Rheumatism* 56: 147-157. DOI: 10.1002/art.22337.

Bonfante HDL, Almeida CDS, Abramo C, Grunewald STF, Levy RA, Teixeira HC (2017) CCL2, CXCL8, CXCL9 and CXCL10 serum levels increase with age but are not altered by treatment with hydroxychloroquine in patients with osteoarthritis of the knees. *International Journal of Rheumatic Diseases* 20: 1958-1964. DOI: 10.1111/1756-185X.12589.

Busby WH, Jr, Yocum SA, Rowland M, Kellner D, Lazerwith S, Sverdrup F, Yates M, Radabaugh M, Clemmons DR (2009) Complement 1s is the serine protease that cleaves IGFBP-5 in human osteoarthritic joint fluid. *Osteoarthritis and Cartilage/OARS, Osteoarthritis Research Society* 17: 547-555. DOI: 10.1016/j.joca.2008.08.004.

Chau M, Dou Z, Baroncelli M, Landman EB, Bendre A, Kanekiyo M, Gkouroganni A, Barnes K, Ottosson L, Nilsson O (2022) The synovial microenvironment suppresses chondrocyte hypertrophy and promotes articular chondrocyte differentiation. *NPJ Regenerative Medicine* 7: 51. DOI: 10.1038/s41536-022-00247-2.

Chou CH, Jain V, Gibson J, Attarian DE, Haraden CA, Yohn CB, Laberge RM, Gregory S, Kraus VB (2020) Synovial cell cross-talk with cartilage plays a major role in the pathogenesis of osteoarthritis. *Scientific Reports* 10: 10868. DOI: 10.1038/s41598-020-67730-y.

de Lange-Brokaar BJE, Ioan-Facsinay A, van Osch GJVM, Zuurmond AM, Schoones J, Toes REM, Huizinga TWJ, Kloppenburg M (2012) Synovial inflammation, immune cells and their cytokines in osteoarthritis: a review. *Osteoarthritis and Cartilage/OARS, Osteoarthritis Research Society* 20: 1484-1499. DOI: 10.1016/j.joca.2012.08.027.

de Lange-Brokaar BJE, Kloppenburg M, Andersen SN, Dorjée AL, Yusuf E, Herb-van Toorn L, Kroon HM, Zuurmond AM, Stojanovic-Susulic V, Bloem JL, Nelissen RGHH, Toes REM, Ioan-Facsinay A (2016) Characterization of synovial mast cells in knee osteoarthritis: association with clinical parameters. *Osteoarthritis and Cartilage/OARS, Osteoarthritis Research Society* 24: 664-671. DOI: 10.1016/j.joca.2015.11.011.

Dreier R, Wallace S, Fuchs S, Bruckner P, Grässel S (2001) Paracrine interactions of chondrocytes and macrophages in cartilage degradation: articular chondrocytes provide factors that activate macrophage-derived pro-

gelatinase B (pro-MMP-9). *Journal of Cell Science* 114: 3813-3822. DOI: 10.1242/jcs.114.21.3813.

Enomoto H, Inoki I, Komiya K, Shiomi T, Ikeda E, Obata KI, Matsumoto H, Toyama Y, Okada Y (2003) Vascular endothelial growth factor isoforms and their receptors are expressed in human osteoarthritic cartilage. *The American Journal of Pathology* 162: 171-181. DOI: 10.1016/s0002-9440(10)63808-4.

Felson DT, Niu J, Neogi T, Goggins J, Nevitt MC, Roemer F, Torner J, Lewis CE, Guermazi A, MOST Investigators Group (2016) Synovitis and the risk of knee osteoarthritis: the MOST Study. *Osteoarthritis and Cartilage/OARS, Osteoarthritis Research Society* 24: 458-464. DOI: 10.1016/j.joca.2015.09.013.

Fernandes TL, Gomoll AH, Lattermann C, Hernandez AJ, Bueno DF, Amano MT (2020) Macrophage: A Potential Target on Cartilage Regeneration. *Frontiers in Immunology* 11: 111. DOI: 10.3389/fimmu.2020.00111.

Fox DB, Warnock JJ, Stoker AM, Luther JK, Cockrell M (2010) Effects of growth factors on equine synovial fibroblasts seeded on synthetic scaffolds for avascular meniscal tissue engineering. *Research in Veterinary Science* 88: 326-332. DOI: 10.1016/j.rvsc.2009.07.015.

Fu W, Chen S, Yang R, Li C, Gao H, Li J, Zhang X (2022) Cellular features of localized microenvironments in human meniscal degeneration: a single-cell transcriptomic study. *eLife* 11: e79585. DOI: 10.7554/eLife.79585.

García-Arnanis I, Guillén MI, Gomar F, Pelletier JP, Martel-Pelletier J, Alcaraz MJ (2010) High mobility group box 1 potentiates the pro-inflammatory effects of interleukin-1 β in osteoarthritic synoviocytes. *Arthritis Research & Therapy* 12: R165. DOI: 10.1186/ar3124.

Gerwin N, Scotti C, Halleux C, Fornaro M, Elliott J, Zhang Y, Johnson K, Shi J, Walter S, Li Y, Jacobi C, Laplanche N, Belaud M, Paul J, Glowacki G, Peters T, Wharton KA, Jr, Vostiar I, Polus F, Kramer I, Guth S, Seroutou A, Choudhury S, Laurent D, Gimbel J, Goldhahn J, Schieker M, Brachat S, Roubenoff R, Kneissel M (2022) Angiopoietin-like 3-derivative LNA043 for cartilage regeneration in osteoarthritis: a randomized phase I trial. *Nature Medicine* 28: 2633-2645. DOI: 10.1038/s41591-022-02059-9.

Gunja NJ, Athanasiou KA (2007) Passage and reversal effects on gene expression of bovine meniscal fibrochondrocytes. *Arthritis Research & Therapy* 9: R93. DOI: 10.1186/ar2293.

Hamasaki M, Terkawi MA, Onodera T, Tian Y, Ebata T, Matsumae G, Alhasan H, Takahashi D, Iwasaki N (2020) Transcriptional profiling of murine macrophages stimulated with cartilage fragments revealed a strategy for treatment of progressive osteoarthritis. *Scientific Reports* 10: 7558. DOI: 10.1038/s41598-020-64515-1.

Hamilton JL, Nagao M, Levine BR, Chen D, Olsen BR, Im HJ (2016) Targeting VEGF and Its Receptors for the Treatment of Osteoarthritis and Associated Pain. *Journal*

of Bone and Mineral Research: the Official Journal of the American Society for Bone and Mineral Research 31: 911-924. DOI: 10.1002/jbmr.2828.

Hatsushika D, Muneta T, Nakamura T, Horie M, Koga H, Nakagawa Y, Tsuji K, Hishikawa S, Kobayashi E, Sekiya I (2014) Repetitive allogeneic intraarticular injections of synovial mesenchymal stem cells promote meniscus regeneration in a porcine massive meniscus defect model. *Osteoarthritis and Cartilage/OARS, Osteoarthritis Research Society* 22: 941-950. DOI: 10.1016/j.joca.2014.04.028.

Haywood L, McWilliams DF, Pearson CI, Gill SE, Ganesan A, Wilson D, Walsh DA (2003) Inflammation and angiogenesis in osteoarthritis. *Arthritis and Rheumatism* 48: 2173-2177. DOI: 10.1002/art.11094.

Im HJ, Sharrocks AD, Lin X, Yan D, Kim J, van Wijnen AJ, Hipskind RA (2009) Basic fibroblast growth factor induces matrix metalloproteinase-13 via ERK MAP kinase-altered phosphorylation and sumoylation of Elk-1 in human adult articular chondrocytes. *Open Access Rheumatology: Research and Reviews* 1: 151-161. DOI: 10.2147/oarr.r.s7527.

Ji Q, Zheng Y, Zhang G, Hu Y, Fan X, Hou Y, Wen L, Li L, Xu Y, Wang Y, Tang F (2019) Single-cell RNA-seq analysis reveals the progression of human osteoarthritis. *Annals of the Rheumatic Diseases* 78: 100-110. DOI: 10.1136/annrheumdis-2017-212863.

Jin S, Guerrero-Juarez CF, Zhang L, Chang I, Ramos R, Kuan CH, Myung P, Plikus MV, Nie Q (2021) Inference and analysis of cell-cell communication using CellChat. *Nature Communications* 12: 1088. DOI: 10.1038/s41467-021-21246-9.

Li C, Liu D, Zhao Y, Ding Y, Hua K (2023) Diverse intratumoral heterogeneity and immune microenvironment of two HPV-related cervical cancer types revealed by single-cell RNA sequencing. *Journal of Medical Virology* 95: e28857. DOI: 10.1002/jmv.28857.

Li J, Wang X, Ruan G, Zhu Z, Ding C (2021a) Sprifermin: a recombinant human fibroblast growth factor 18 for the treatment of knee osteoarthritis. *Expert Opinion on Investigational Drugs* 30: 923-930. DOI: 10.1080/13543784.2021.1972970.

Li Z, Huang Z, Bai L (2021b) Cell Interplay in Osteoarthritis. *Frontiers in Cell and Developmental Biology* 9: 720477. DOI: 10.3389/fcell.2021.720477.

Liao L, Chen Y, Wang W (2016) The current progress in understanding the molecular functions and mechanisms of visfatin in osteoarthritis. *Journal of Bone and Mineral Metabolism* 34: 485-490. DOI: 10.1007/s00774-016-0743-1.

MacKinnon AC, Farnworth SL, Hodkinson PS, Henderson NC, Atkinson KM, Leffler H, Nilsson UJ, Haslett C, Forbes SJ, Sethi T (2008) Regulation of alternative macrophage activation by galectin-3. *Journal of Immunology (Baltimore, Md.: 1950)* 180: 2650-2658. DOI:

10.4049/jimmunol.180.4.2650.

Maglaviceanu A, Wu B, Kapoor M (2021) Fibroblast-like synoviocytes: Role in synovial fibrosis associated with osteoarthritis. *Wound Repair and Regeneration: Official Publication of the Wound Healing Society [and] the European Tissue Repair Society* 29: 642-649. DOI: 10.1111/wrr.12939.

Martel-Pelletier J, Di Battista JA, Lajeunesse D, Pelletier JP (1998) IGF/IGFBP axis in cartilage and bone in osteoarthritis pathogenesis. *Inflammation Research: Official Journal of the European Histamine Research Society ... [et al.]* 47: 90-100. DOI: 10.1007/s000110050288.

Maruyama K, Muramatsu H, Ishiguro N, Muramatsu T (2004) Midkine, a heparin-binding growth factor, is fundamentally involved in the pathogenesis of rheumatoid arthritis. *Arthritis and Rheumatism* 50: 1420-1429. DOI: 10.1002/art.20175.

Micheroli R, Elhai M, Edalat S, Frank-Bertoncelj M, Bürki K, Ciurea A, MacDonald L, Kurowska-Stolarska M, Lewis MJ, Goldmann K, Cubuk C, Kuret T, Distler O, Pitzalis C, Ospelt C (2022) Role of synovial fibroblast subsets across synovial pathotypes in rheumatoid arthritis: a deconvolution analysis. *RMD Open* 8: e001949. DOI: 10.1136/rmdopen-2021-001949.

Morales TI (2008) The quantitative and functional relation between insulin-like growth factor-I (IGF) and IGF-binding proteins during human osteoarthritis. *Journal of Orthopaedic Research: Official Publication of the Orthopaedic Research Society* 26: 465-474. DOI: 10.1002/jor.20549.

Mosser DM (2003) The many faces of macrophage activation. *Journal of Leukocyte Biology* 73: 209-212. DOI: 10.1189/jlb.0602325.

Murata M, Yudoh K, Masuko K (2008) The potential role of vascular endothelial growth factor (VEGF) in cartilage: how the angiogenic factor could be involved in the pathogenesis of osteoarthritis? *Osteoarthritis and Cartilage/OARS, Osteoarthritis Research Society* 16: 279-286. DOI: 10.1016/j.joca.2007.09.003.

Nishiyama S, Hirose N, Yanoshita M, Takano M, Kubo N, Yamauchi Y, Onishi A, Ito S, Sakata S, Kita D, Asakawa-Tanne Y, Tanimoto K (2021) ANGPTL2 Induces Synovial Inflammation via LILRB2. *Inflammation* 44: 1108-1118. DOI: 10.1007/s10753-020-01406-7.

Okubo M, Kimura T, Fujita Y, Mochizuki S, Niki Y, Enomoto H, Suda Y, Toyama Y, Okada Y (2011) Semaphorin 3A is expressed in human osteoarthritic cartilage and antagonizes vascular endothelial growth factor 165-promoted chondrocyte migration: an implication for chondrocyte cloning. *Arthritis and Rheumatism* 63: 3000-3009. DOI: 10.1002/art.30482.

Pufe T, Bartscher M, Petersen W, Tillmann B, Mentlein R (2003) Pleiotrophin, an embryonic differentiation and growth factor, is expressed in osteoarthritis. *Osteoarthritis and Cartilage/OARS, Osteoarthritis*

Research Society 11: 260-264. DOI: 10.1016/s1063-4584(02)00385-0.

Pufe T, Harde V, Petersen W, Goldring MB, Tillmann B, Mentlein R (2004) Vascular endothelial growth factor (VEGF) induces matrix metalloproteinase expression in immortalized chondrocytes. *The Journal of Pathology* 202: 367-374. DOI: 10.1002/path.1527.

Qu D, Zhu JP, Childs HR, Lu HH (2019) Nanofiber-based transforming growth factor- β 3 release induces fibrochondrogenic differentiation of stem cells. *Acta Biomaterialia* 93: 111-122. DOI: 10.1016/j.actbio.2019.03.019.

Roemer FW, Kassim Javaid M, Guermazi A, Thomas M, Kiran A, Keen R, King L, Arden NK (2010) Anatomical distribution of synovitis in knee osteoarthritis and its association with joint effusion assessed on non-enhanced and contrast-enhanced MRI. *Osteoarthritis and Cartilage/OARS, Osteoarthritis Research Society* 18: 1269-1274. DOI: 10.1016/j.joca.2010.07.008.

Sakaguchi Y, Sekiya I, Yagishita K, Muneta T (2005) Comparison of human stem cells derived from various mesenchymal tissues: superiority of synovium as a cell source. *Arthritis and Rheumatism* 52: 2521-2529. DOI: 10.1002/art.21212.

Sanchez-Lopez E, Coras R, Torres A, Lane NE, Guma M (2022) Synovial inflammation in osteoarthritis progression. *Nature Reviews. Rheumatology* 18: 258-275. DOI: 10.1038/s41584-022-00749-9.

Sarmanova A, Hall M, Moses J, Doherty M, Zhang W (2016) Synovial changes detected by ultrasound in people with knee osteoarthritis - a meta-analysis of observational studies. *Osteoarthritis and Cartilage/OARS, Osteoarthritis Research Society* 24: 1376-1383. DOI: 10.1016/j.joca.2016.03.004.

Sica A, Mantovani A (2012) Macrophage plasticity and polarization: *in vivo* veritas. *The Journal of Clinical Investigation* 122: 787-795. DOI: 10.1172/JCI59643.

Silverstein AM, Stefani RM, Sobczak E, Tong EL, Atur MG, Shah RP, Bulinski JC, Ateshian GA, Hung CT (2017) Toward understanding the role of cartilage particulates in synovial inflammation. *Osteoarthritis and Cartilage/OARS, Osteoarthritis Research Society* 25: 1353-1361. DOI: 10.1016/j.joca.2017.03.015.

Smith MD, Triantafillou S, Parker A, Youssef PP, Coleman M (1997) Synovial membrane inflammation and cytokine production in patients with early osteoarthritis. *The Journal of Rheumatology* 24: 365-371.

Song X, Xie Y, Liu Y, Shao M, Wang W (2015) Beneficial effects of coculturing synovial derived mesenchymal stem cells with meniscus fibrochondrocytes are mediated by fibroblast growth factor 1: increased proliferation and collagen synthesis. *Stem Cells International* 2015: 926325. DOI: 10.1155/2015/926325.

Steinhagen J, Bruns J, Niggemeyer O, Fuerst M, Rütter W, Schünke M, Kurz B (2010) Perfusion culture system: Synovial fibroblasts modulate articular chondro-

cyte matrix synthesis *in vitro*. *Tissue & Cell* 42: 151-157. DOI: 10.1016/j.tice.2010.03.003.

Stuart T, Butler A, Hoffman P, Hafemeister C, Papalexi E, Mauck WM, 3rd, Hao Y, Stoekius M, Smibert P, Satija R (2019) Comprehensive Integration of Single-Cell Data. *Cell* 177: 1888-1902.e21. DOI: 10.1016/j.cell.2019.05.031.

Su W, Liu G, Liu X, Zhou Y, Sun Q, Zhen G, Wang X, Hu Y, Gao P, Demehri S, Cao X, Wan M (2020) Angiogenesis stimulated by elevated PDGF-BB in subchondral bone contributes to osteoarthritis development. *JCI Insight* 5: e135446. DOI: 10.1172/jci.insight.135446.

Suleiman L, Négrier C, Boukerche H (2013) Protein S: A multifunctional anticoagulant vitamin K-dependent protein at the crossroads of coagulation, inflammation, angiogenesis, and cancer. *Critical Reviews in Oncology/Hematology* 88: 637-654. DOI: 10.1016/j.critrevonc.2013.07.004.

Sun H, Wen X, Li H, Wu P, Gu M, Zhao X, Zhang Z, Hu S, Mao G, Ma R, Liao W, Zhang Z (2020) Single-cell RNA-seq analysis identifies meniscus progenitors and reveals the progression of meniscus degeneration. *Annals of the Rheumatic Diseases* 79: 408-417. DOI: 10.1136/annrheumdis-2019-215926.

Takata K, Uchida K, Takano S, Mukai M, Inoue G, Sekiguchi H, Aikawa J, Miyagi M, Iwase D, Takaso M (2021) Possible Regulation of bFGF Expression by Mast Cells in Osteoarthritis Patients with Obesity: A Cross-Sectional Study. *Diabetes, Metabolic Syndrome and Obesity: Targets and Therapy* 14: 3291-3297. DOI: 10.2147/DMSO.S319537.

Toegel S, Weinmann D, André S, Walzer SM, Bilban M, Schmidt S, Chiari C, Windhager R, Krall C, Bennani-Baiti IM, Gabius HJ (2016) Galectin-1 Couples Glycobiology to Inflammation in Osteoarthritis through the Activation of an NF- κ B-Regulated Gene Network. *Journal of Immunology (Baltimore, Md.: 1950)* 196: 1910-1921. DOI: 10.4049/jimmunol.1501165.

Tsai CH, Liu SC, Chung WH, Wang SW, Wu MH, Tang CH (2020) Visfatin Increases VEGF-dependent Angiogenesis of Endothelial Progenitor Cells during Osteoarthritis Progression. *Cells* 9: 1315. DOI: 10.3390/cells9051315.

Unver N, Esendagli G, Yilmaz G, Guc D (2015) CXCL7-induced macrophage infiltration in lung tumor is independent of CXCR2 expression: CXCL7-induced macrophage chemotaxis in LLC tumors. *Cytokine* 75: 330-337. DOI: 10.1016/j.cyto.2015.07.018.

Wei K, Korsunsky I, Marshall JL, Gao A, Watts GFM, Major T, Croft AP, Watts J, Blazar PE, Lange JK, Thornhill TS, Filer A, Raza K, Donlin LT, Accelerating Medicines Partnership Rheumatoid Arthritis & Systemic Lupus Erythematosus (AMP RA/SLE) Consortium, Siebel CW, Buckley CD, Raychaudhuri S, Brenner MB (2020) Notch signalling drives synovial fibroblast iden-

tity and arthritis pathology. *Nature* 582: 259-264. DOI: 10.1038/s41586-020-2222-z.

Weinmann D, André S, Walzer S, Chiari C, Bennani-Baiti IM, Windhager R, Gabius HJ, Toegel S (2016) Galectin-1 induces inflammation and cartilage degeneration in osteoarthritis through NF- κ B-signaling. *Osteoarthritis and Cartilage* 24: S139-S140. DOI: 10.1016/j.joca.2016.01.274.

Weinmann D, Kenn M, Schmidt S, Schmidt K, Walzer SM, Kubista B, Windhager R, Schreiner W, Toegel S, Gabius HJ (2018) Galectin-8 induces functional disease markers in human osteoarthritis and cooperates with galectins-1 and -3. *Cellular and Molecular Life Sciences: CMLS* 75: 4187-4205. DOI: 10.1007/s00018-018-2856-2.

Whitley CB, Langer LO, Jr, Ophoven J, Gilbert EF, Gonzalez CH, Mammel M, Coleman M, Roseberg S, Rodrigues CJ, Sibley R (1984) Fibrochondrogenesis: lethal, autosomal recessive chondrodysplasia with distinctive cartilage histopathology. *American Journal of Medical Genetics* 19: 265-275. DOI: 10.1002/ajmg.1320190209.

Wu S, Singh S, Varney ML, Kindle S, Singh RK (2012) Modulation of CXCL-8 expression in human melanoma cells regulates tumor growth, angiogenesis, invasion, and metastasis. *Cancer Medicine* 1: 306-317. DOI: 10.1002/cam4.28.

Wu Y, Yang S, Ma J, Chen Z, Song G, Rao D, Cheng Y, Huang S, Liu Y, Jiang S, Liu J, Huang X, Wang X, Qiu S, Xu J, Xi R, Bai F, Zhou J, Fan J, Zhang X, Gao Q (2022) Spatiotemporal Immune Landscape of Colorectal Cancer Liver Metastasis at Single-Cell Level. *Cancer Discovery* 12: 134-153. DOI: 10.1158/2159-8290.CD-21-0316.

Yu G, Wang LG, Han Y, He QY (2012) clusterProfiler: an R package for comparing biological themes among gene clusters. *Omic: a Journal of Integrative Biology* 16: 284-287. DOI: 10.1089/omi.2011.0118.

Zhang F, Wei K, Slowikowski K, Fonseka CY, Rao DA, Kelly S, Goodman SM, Tabechian D, Hughes LB, Salomon-Escoto K, Watts GFM, Jonsson AH, Rangel-Moreno J, Meednu N, Roza C, Apruzzese W, Eisenhaure TM, Lieb DJ, Boyle DL, Mandelin AM, 2nd, Accelerating Medicines Partnership Rheumatoid Arthritis and Systemic Lupus Erythematosus (AMP RA/SLE) Consortium, Boyce BF, DiCarlo E, Gravalles EM, Gregersen PK, Moreland L, Firestein GS, Hachohen N, Nusbaum C, Lederer JA, Perlman H, Pitzalis C, Filer A, Holers VM, Bykerk VP, Donlin LT, Anolik JH, Brenner MB, Raychaudhuri S (2019) Defining inflammatory cell states in rheumatoid arthritis joint synovial tissues by integrating single-cell transcriptomics and mass cytometry. *Nature Immunology* 20: 928-942. DOI: 10.1038/s41590-019-0378-1.

Zhou C, Zheng H, Seol D, Yu Y, Martin JA (2014) Gene expression profiles reveal that chondrogenic progenitor cells and synovial cells are closely related. *Journal of Orthopaedic Research: Official Publication of the Orthopaedic Research Society* 32: 981-988. DOI:

10.1002/jor.22641.

Zhu Z, Xie J, Manandhar U, Yao X, Bian Y, Zhang B (2021) RNA binding protein GNL3 up-regulates IL24 and PTN to promote the development of osteoarthritis. *Life Sci-*

ences 267: 118926. DOI: [10.1016/j.lfs.2020.118926](https://doi.org/10.1016/j.lfs.2020.118926).

Editor's note: The Scientific Editor responsible for this paper was Brian Johnstone.